Russian Original Vol. 13, No. 9, September, 1970
May 15, 1973

RPQEAC 13(9) 981-1102 (1970)

RADIOPHYSICS AND QUANTUM ELECTRONICS

ИЗВЕСТИЯ ВУЗ. РАДИОФИЗИКА
(IZVESTIYA VUZ. RADIOFIZIKA)

TRANSLATED FROM RUSSIAN

CONSULTANTS BUREAU, NEW YORK

THERMAL RADIATION FROM THE MOON AND THE PHYSICAL PROPERTIES OF THE UPPER LUNAR LAYER

A REVIEW

V. S. Troitskii and T. V. Tikhonova

UDC 532.164.34

TABLE OF CONTENTS

Scientific-Research Institute of Radiophysics, Gor'kii University. Translated from Izvestiya Vysshikh Uchebnykh Zavedenii, Radiofizika, Vol. 13, No. 9, pp. 1273-1311, September, 1970. Original article submitted December 3, 1969.

1. Introduction

The present review is a critical generalization of Soviet and foreign investigations of the moon according to its intrinsic radiation in the range of infrared and radio waves with resort to radar data and laboratory investigations of the electrical and thermal properties of the terrestrial analogs of the substance forming the upper layer of the moon. *

Before 1927 the only source of information on physical conditions on the moon were optical observations which yielded information on the state of matter on the actual surface only. From 1927 to 1930 Pettit and Nicholson [1] performed the first measurements of the intrinsic radiation from the moon at infrared wavelengths during lunations and eclipses. These measurements allowed the surface temperature of the planet to be determined, an estimate of the thermal conductivity of the lunar substance, and the first conclusions to be formed on the structure of the lunar substance.

In 1946 measurements of the intrinsic radio emission from the moon $\lambda = 1.25$ cm were carried out [2]. Since then an enormous amount of experimental material has been obtained on the intrinsic radio emission from the moon over a wide range of wavelengths. On the basis of these investigations, together with the data of radar and infrared measurements obtained principally abroad, a picture of the physical conditions on the moon can be drawn that is fairly complete and free from internal contradictions. A generalization of the results obtained before 1965 is presented in [3-5], while a generalization of the results obtained up to 1967 is given in [6]. The purpose of the present review is to perform a certain summing up of lunar research on intrinsic radiation and reflection of radio waves from the lunar surface, to present a modern model of the structure of the upper layer of the moon on the basis of available experimental data, and to develop methods of their interpretation.

II. Theory of the Thermal Mode of the Surface

1. General Relationships. The principal features of lunar radio emission, which is thermal in character, are determined by the conditions governing the heating of the lunar surface by solar radiation. The thermal mode of the lunar surface and the depth distribution of the temperature can be described by the thermal conductivity equation with the appropriate boundary and initial conditions:

$$\frac{\partial}{\partial y}\left[k(y, T)\frac{\partial T}{\partial y}\right] = \rho(y)\, c(y, T)\frac{\partial T}{\partial t}. \tag{1}$$

In the case of a periodic thermal mode (lunation) the boundary conditions have the form

$$\left(k_s\frac{\partial T}{\partial y}\right)_{y=0} = \sigma(1 - R_{IR})[T(0, t)]^4 + q - \begin{cases} S_0(1-R_l)\cos\psi\cos(\Omega t-\varphi) & \left(|\Omega t - \varphi| \leqslant \frac{\pi}{2}\right) \\ 0 & \left(\frac{\pi}{2} < (\Omega t - \varphi) < \frac{3\pi}{2}\right) \end{cases}, \tag{2}$$

while for a nonperiodic mode (eclipses) they have the form

$$\left(k_s\frac{\partial T}{\partial y}\right)_{y=0} = \sigma(1 - R_{IR})[T(0, t)]^4 + q - S_0(1 - R_l)\cos\psi\cos\varphi\, f(t). \tag{3}$$

In Eqs. (1)-(3) $\rho(y)$ is the density of the lunar substance; c(y, T) is the specific heat; q is the density of the heat flux from the interior of the moon; σ is the Stefan–Boltzmann constant; R_l and R_{IR} are respectively the light and infrared albedos of the surface; S_0 is the solar constant; f(t) is the function for the flux variation during an eclipse; φ and ψ are respectively the longitude and latitude of the surface element whose

*It seems natural to the authors that the review expresses the point of view developed by the associates of the Gor'kii Scientific-Research Radiophysics Institute where many theoretical and experimental investigations have been performed.

thermal mode is being considered; Ω is the frequency of lunations; $k(y, T) = k_0 + k_r$ is the total thermal conductivity and is equal to the sum of the molecular k_0 and radiation k_r thermal conductivities; $k_s = k_0 + k_{rs}$; k_{rs} is the radiation thermal conductivity of the surface.

As shown in [7], in the presence of radiation thermal conductivity in a solid porous body transparent to infrared waves, the heat transfer equation and the boundary condition contain different radiation thermal conductivity coefficients. It turns out that k_{rs} in the boundary condition is $2n^2/(1-R_i)f(n)$ times as small as k_r in the differential equation, where n, R_i are respectively the refractive index and reflection coefficient of infrared waves in the body and $f(n) = n^2[1-(1-1/n^2)^{3/2}]$. The initial conditions in the case of calculating the lunation mode are arbitrary by virtue of the fact that the steady-state constrained periodic solution is sought. In the case of an eclipse the initial conditions are determined by the temperature distribution before the beginning of the eclipse. Since the eclipses occur only at full moon, it follows that this temperature distribution is obtained as the solution of the equation of the thermal conductivity for the lunation mode at time $t = 0$.

Problems on the investigation of the thermal mode during lunations and eclipses may be separated into two types.

1) The solution of Eq. (1) with the boundary conditions (2) or (3), when the fluxes of solar energy S_0 or $S_0 f(t)$ are assumed to be stipulated. The solutions of problems of this type cannot be obtained analytically; they are calculated on an electronic computer.

2) The solution of Eq. (1) for a stipulated surface temperature. During lunations the insolation is periodic in character, and therefore the most convenient representation for the surface temperature is a function in the form of a Fourier series. To a sufficiently good approximation, the curve for the variation of the surface temperature during an eclipse may be represented by four linear segments. The solution of problems of this type allows an analytic expression to be derived for the depth distribution of the temperature whose knowledge is necessary in calculating lunar radio emission.

2. The Thermal Modes during Lunations. The Homogeneous Model of the Surface Layer. In order to calculate the thermal mode of the surface it is necessary to adopt some model of the structure of the upper layer. As a first approximation the homogeneous model was chosen in which the properties of the substance do not vary with depth and are independent of temperature. It turns out that in this case the surface temperature depends only on a single parameter $\gamma = (k\rho c)^{-1/2}$.

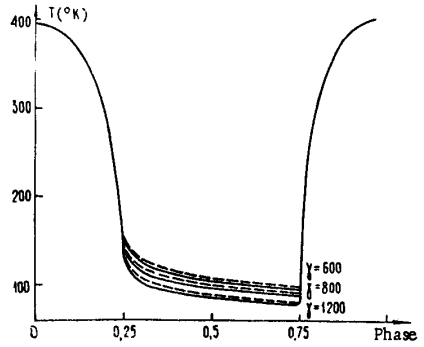

Fig. 1

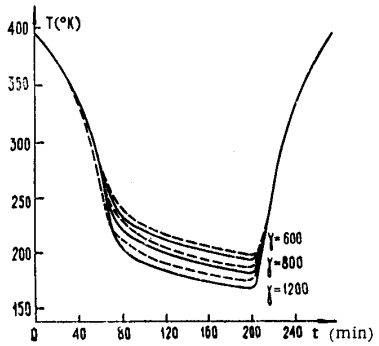

Fig. 2

Fig. 1. Temperature variation of the surface at the center of the lunar disk as a function of phase for the parameter values γ = 600; 800; 1200. The solid curves are for the homogeneous model without consideration of the dependence of the properties of the substance on temperature; the dashed curves are with allowance for this dependence.

Fig. 2. Temperature variation of the surface at the center of the lunar disk during an eclipse for γ = 600; 800; 1200. The solid curves neglect the temperature dependence of the properties of the substance; the dashed curves take this dependence into account.

The problem of the first type for the homogeneous model of the structure of the upper layer was first considered by Wesselink [8], and then in greater detail by Jaeger [9]. In order to determine the temperature variation of the surface at the center of the lunar disk, Jaeger solved the thermal conductivity equation (1) for the boundary condition (2) using the method of numerical integration.

In [10, 11] the temperature mode of the lunar surface was investigated in greater detail using the latest data on the magnitude of the solar constant. Figure 1 displays the dependence of the surface temperature at the center of the lunar disk on the phase angle (solid curves), obtained by solving (1) and (2) on an electronic computer for various values of the parameter γ.

The results of calculating the surface temperature are represented in the form

$$T(\varphi, \psi, t) = T_0(\psi) + \sum_{n=1}^{\infty} (-1)^{\alpha_n} T_n(\psi) \cos(n\Omega t - n\varphi - \varphi_n), \tag{4}$$

where φ_n is the phase shift of the n-th harmonic of the surface-temperature variation relative to the phase of the incident flux. As demonstrated in [10], the first five harmonics $T_n(\varphi)$ can be approximated well by the expressions

$$\begin{aligned} T_0(\psi) &= T_0(0)\cos^{0,25}\psi, & T_3(\psi) &= T_3(0)\cos^{0,44}\psi, \\ T_1(\psi) &= T_1(0)\cos^{0,33}\psi, & T_4(\psi) &= T_4(0)\cos^{0,3}\psi, \\ T_2(\psi) &= T_2(0)\cos^{0,27}\psi, \end{aligned} \tag{5}$$

while the sign of these harmonics is determined by the index $\alpha_n = (n-1)(n-2)/2$.

The problem of the second type for the same homogeneous model of the structure of the upper layer was solved analytically in [72]. The solution of the thermal conductivity equation (1) for the boundary condition (4) leads to the following expression for the depth distribution of the temperature at any point of the lunar surface having the coordinates (φ, ψ):

$$T(y, \varphi, \psi, t) = T_0(\psi) + \sum_{n=1}^{\infty} (-1)^{\alpha_n} T_n(\psi) \exp\left(-y\sqrt{\frac{n\Omega\rho c}{2k}}\right) \cos\left(n\Omega t - n\varphi - \varphi_n - y\sqrt{\frac{n\Omega\rho c}{2k}}\right). \tag{6}$$

The temperature at any depth is made up of a constant component and an alternating component formed by the sum of harmonics having periods that are multiples of the lunation period ($\tau = 2\pi/\Omega = 29.5$ earth days). Each of the harmonics decays with depth, the amplitude of the temperature oscillations decreasing by a factor e compared with the surface value at a depth $l_{Tn} = \sqrt{2k/n\Omega\rho c}$. This value has been called the penetration depth of the temperature wave. It characterizes the thickness of the surface layer heated by the sun during a lunar day. At a depth exceeding l_T by a factor of three to four the temperature oscillations are practically absent.

The homogeneous model with a thermal conductivity and specific heat that depend on temperature was considered in the second approximation. As is well known, the thermal conductivity of porous bodies depends on temperature due to the radiative heat transfer through the pores. In the "lunar" temperature interval the radiant transfer is achieved via radiation at infrared wavelengths corresponding to the Planck maximum $\lambda = 0.38/T \simeq 10$-$30\ \mu$. For a porous body in which the effective dimension of the pores is equal to l_n, while the substance itself is opaque to infrared waves, the magnitude of the radiation thermal conductivity k_r is equal to

$$k_{rn} = \frac{R_{IR}}{2 - R_{IR}} 4\sigma l_n T^3. \tag{7}$$

If infrared waves penetrate into the substance, then $k_r = (16/3)\sigma\varepsilon_n\bar{l}_\nu T^3$, where $\bar{l}_\nu$ is the Rosseland average penetration depth of the infrared radiation into the substance; ε_n is the dielectric constant of the substance in the infrared range.

Calculations show that for the dependence $\bar{l}_\nu = a\lambda$ (which derives from radio measurements and the theory of nonresonance absorption of waves in matter), $\bar{l}_\nu = 0.365\ a/T$. Hence [13]

$$k_r = 2\varepsilon_{IR} a \sigma T^3. \tag{8}$$

The total thermal conductivity is equal to the sum of the molecular and radiation thermal conductivities.

Jaeger [9] was the first to analyze the thermal mode of the moon with allowance for radiation thermal conductivity, but the calculation did not produce any substantial changes in the dependence of the temperature on phase.

In the paper by Ingrao, Young and Linsky [14] results were presented of calculations of the lunar surface temperature during lunations and eclipses for the homogeneous and two-layer models with allowance for the temperature dependence of the thermal conductivity (the specific heat was assumed constant). In [14] likewise, calculations are given for the Muncey model [15] in which the dependence of the specific heat and thermal conductivity on temperature was assumed to be linear. It turned out that the character of the temperature drop during the setting of the sun satisfied both the Muncey model and the model with radiation thermal conductivity of the form $k_r = BT^3$. In the first case agreement with experiment is obtained for $\gamma = 400$-450, $T = 350°$, while in the second case it is obtained for $\gamma = 600$.

Further on the authors of [14] note that within the framework of the two models indicated there are certain differences in the depth distribution of the temperature to the extent of several centimeters, and as a result there may be differences in the radio emission in the millimeter range of wavelengths.

However, as estimates show, this difference is very small and cannot be detected in experiments that yield the phase variation of the radiation in view of the insufficient accuracy of these measurements.

The problem of the effect of the temperature dependence of the specific heat and thermal conductivity on the thermal mode and the radio-emission spectrum of the moon was considered in detail in [11]. Equation (1) with the boundary condition (2) was solved on an electronic computer on the assumption that the dependence of the specific heat on temperature is the same for the substance of the upper layer of the moon as it is for terrestrial rocks, while the thermal conductivity is independent of temperature. Calculations show that consideration of the temperature dependence of the specific heat leads to a somewhat deeper cooling of the lunar surface in the absence of insolation.

Further on in [11] the perturbation method is used to obtain the analytic solution of Eq. (1) for the boundary condition (4) in the case when the specific heat $c = \text{const}$, while the thermal conductivity $k = k_0(1 + B_nT^n)$ where $n = 1, 2, 3$ and $B_nT^n < 1$ throughout the interval of lunar temperatures. The expression for the depth distribution of the temperature at the center of the lunar disk has the following form in this case:

$$T(y, t) = T_0 + \frac{n}{4} B_n T_0^{n-1} T_1^2 (1 - e^{-2\beta y}) + T_1 e^{-\beta y} \cos(\Omega t - \varphi - \beta y)\left(1 + \frac{\beta B_n T_0^{n-1}}{2} y\right). \quad (9)$$

From Eq. (9) it follows that the temperature dependence of the thermal conductivity (first shown in [33]) leads to a growth of the constant component of the temperature with depth due to a special effect of detection of the temperature wave propagating in a nonlinear medium.

In order to estimate the accuracy of the approximate analytic solution (9) the exact solution of Eq. (1) with the boundary condition (3) was obtained on an electronic computer [11] for the center of the lunar disk when the specific heat and thermal conductivity depend on temperature as follows:

$$c = c_0 T, \qquad k = k_0(1 + B_n T^n).$$

A comparison of the exact and approximate solutions yielded good agreement.

Figure 1 displays the dependence of the temperature at the center of the disk on the local phase (dashed curves) for various γ and $BT^3 = 0.5$. A comparison of these curves and those for temperature-independent properties of the substance (the solid curves) shows that consideration of the effect of the temperature dependences of the specific heat and thermal conductivity does not yield changes of the surface temperature larger than the overall accuracy of the analysis and experiment.

In order to estimate the radiative-transfer function it is necessary to find phenomena which to a sufficiently strong degree determine the dependence of the thermal conductivity on temperature. It turned out that such a phenomenon exists. As is evident from Eq. (9), the constant component of the true temperature increases with depth according to the law

$$T_0(y) = T_0 + \Delta T_{max}(1 - e^{-2y/l_T}), \quad (10)$$

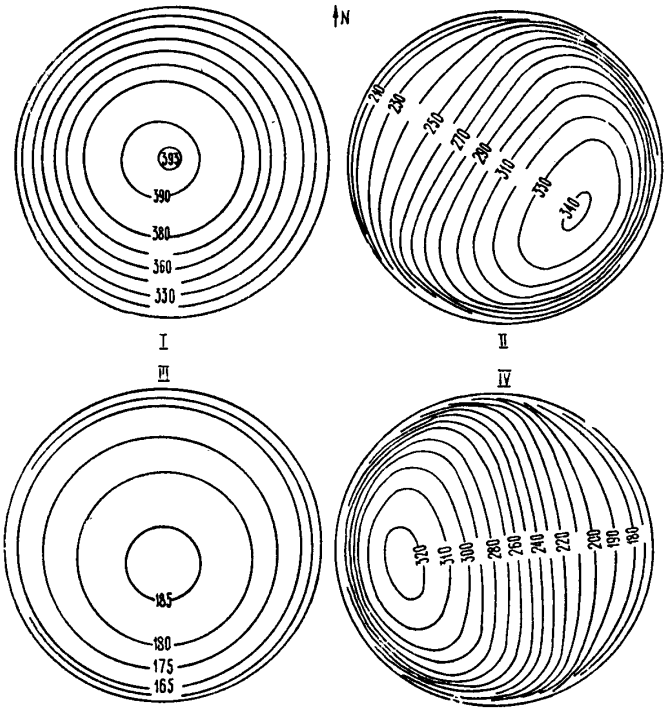

Fig. 3. Temperature distribution over the visible lunar disk for the eclipse times 0, 100, 190, and 290 minutes.

where ΔT_{max} depends on γ and the quantity k_r. An increase in temperature with depth leads to the growth of the constant component of the lunar radio emission as the wavelength increases. From the calculations it follows that the constant component of the brightness temperature of the radio emission depends on wavelength according to the law [11]

$$T_{e0} \simeq T_0 + \Delta T_{max} \frac{2\delta}{1+2\delta}. \tag{11}$$

As will be demonstrated below, for the moon $\delta = 2.3\lambda$. This means that at wavelengths of the order of 2-3 cm the constant component already reaches the practically maximum value 2-3 cm. Thus, by measuring the temperature on the surface (in infrared waves) and in the interior (at wavelengths $\lambda \simeq$ 2-3 cm), one can find the temperature increment ΔT_{max} and determine k_r/k_0.

Such a determination became possible due to precision measurements of radio temperature by the "artificial moon" method. In [13] it was shown that the existing difference (10-15°) between the constant components as obtained by infrared measurements and radio measurements can be explained by the effects considered. By comparison with the theory it was found that if the lunar substance is opaque to infrared waves and has $\gamma \simeq 800$ cal$^{-1}\cdot$cm$^2\cdot$sec$^{1/2}\cdot$deg, then the relative fraction of radiative transfer through the pores at T = 300°K is equal to $k_{rn}(300)/k_0 = 0.25$. For a permeable substance $k_r(300)/k_0 = 0.4$. Analogous numerical calculations were also carried out in [129].

In [9, 72] in addition to the homogeneous model the two-layer model of the surface layer was considered; according to the two-layer model the lunar surface is represented as consisting of silicate rock with a low value of the thermal parameter $\gamma \simeq 100$, covered with a thin layer of dust for which $\gamma = 1000$. However, as further investigations of the lunar radio emission showed, its surface layer has a quasihomogeneous structure in its interior, while the abruptly-inhomogeneous model must be rejected as not corresponding to the experimental data [16].

3. The Thermal Mode of the Surface during Eclipse. The first numerical calculation of the lunar surface temperature during an eclipse was carried out by Jaeger [9]. Equation (1) was solved for the boundary condition (3) on the assumption that the properties of the substance do not change with depth and do not depend on temperature. A calculation of the thermal mode of the surface element at the center of the lunar disk for the circumstances of the eclipse of 1963 is presented in [11], assuming dependence of the specific heat on temperature in the form $c = c_0T$ and dependence of the thermal conductivity on temperature in the form $k = k_0(1 + BT^3)$.

Figure 2 displays the dependence of the surface temperature during the eclipse for $BT^3 = 0.5$ (the dashed curves), as obtained by the method of solving Eq. (1) with the boundary condition (3). (The solid curves correspond to the case when the properties of the substance do not depend on temperature.)

The calculations of [9, 11] showed that both in the case of lunations and in the case of eclipses the presence of the dependences c(T) and k(T) of the lunar substance has little effect on the thermal mode of the lunar surface. This provides the basis for assuming c = const and k = const in determining the surface distribution of the temperature. The results of calculating the temperature distribution over the visible lunar disk [17] for four moments during the eclipse are displayed in Fig. 3. The estimates show that the temperature mode of the surface is almost completely restored two hours after the end of the eclipse.

In order to develop the theory of radio emission during an eclipse it is necessary to know the temperature distribution with depth T(y, t). The analytic solution of the problem of the lunar thermal mode during an eclipse was obtained in [18, 19]. However, in [18] the initial temperature distribution T(y, 0) is not taken into account in solving the thermal conductivity equation. In [19] the problem is solved on the assumption that the upper layer is homogeneous in its properties down to the depth where temperature oscillations may still be present during the eclipse, and furthermore the properties of the substance do not depend on temperature. The temperature of the surface element is assumed known at any time during the eclipse. Actually, the curve for the temperature variation of the surface during the eclipse is known from a number of measurements (see, for example, [20]). It may be approximated fairly well by four linear segments confined between the characteristic times t_k of the eclipse:

$$T(0, t) = T_k + \alpha_k(t - t_k), \quad \alpha_k = \frac{T_{k+1} - T_k}{t_{k+1} - t_k}, \quad \alpha_4 = 0$$
$$(k = 1, 2, 3, 4).$$

Here t_1 is the instant corresponding to the beginning of the half-shadow phase of the eclipse; t_2 is the beginning of the shadow phase; t_3 is the end of the shadow phase and the beginning of the half-shadow phase; t_4 is the end of the half-shadow phase; T_k is the surface temperature corresponding to the time t_k. As the initial condition we use the temperature distribution (6) obtained from the solution of the thermal problem during lunation for the center of the disk ($\psi = 0$, $\varphi = 0$) and time t = 0 (full moon).

4. The Effect of Surface Roughness on Its Thermal Mode. It follows from a theoretical analysis that the thermal mode of the lunar surface that the temperature distribution along the smooth disk of the totally illuminated moon can be described by the law

$$T = T_0 \cos^{1/4}\psi. \tag{12}$$

However, even the early results obtained by Pettit and Nicholson [1] were approximated well by an expression of the form

$$T = T_0 \cos^{1/6}\psi. \tag{13}$$

This difference between (12) and (13) was explained by the authors on the basis of the roughness of the surface.

Recent measurements of the temperature distribution along the illuminated disk, which were performed with a high resolution during lunations in the far infrared and visible ranges [21], yielded an analogous result. They allowed patterns of isotherms to be obtained from which it can be seen that the temperature of a surface element depends both on the height of the sun and on the observation angle. These measurements substantiated the fact that the temperature distribution over the surface has the form (13). Moreover, they substantiated the anomaly in the temperature variation of the subsolar point: when the subsolar point moves toward the edge of the disk its temperature decreases. Evidently, the principal contribution to these effects is made by the surface roughness. In the literature two

types of profiles are considered in this connection: profiles with small-scale inhomogeneities ranging from a millimeter to several centimeters, and profiles with large-scale irregularities of the order of a meter or more.

Anomalies in the temperature variation of the subsolar point are explained in [22] by means of the wavy-surface model. It is shown that if the dimensions of the irregularities are of the order of millimeters and centimeters, then for normal incidence of solar rays relative to an observer looking at the surface of a certain angle the temperature of this surface will be somewhat lower than the temperature of a flat surface consisting of the same material. In [23] the same effect is explained by means of spherical denser craters having centimeter dimensions.

The anomalies in the brightness distribution over the lunar disk are explained on the basis of large-scale inhomogeneities. Under these conditions it is the usual practice to consider the model in which the height fluctuations are distributed according to a normal law, while the horizontal dimensions of the inhomogeneities are described by an autocorrelation function of exponential form [24, 25]. A comparison of the theoretical computations of Smith [25] with the experimental results obtained by Ingrao, Young and Linsky [26], and also by Saary and Shorthill [21] allows the magnitude of the mean-square slope of the roughness to be estimated. This magnitude turns out to equal 20°. An attempt to explain the anomalies in the brightness of the subsolar point using the same analysis leads to a highly exaggerated value of the mean-square slope (60-70°), which places the assumptions on which the analysis was made in doubt.

The literature discusses another fact which may evidently help in explaining these phenomena: the presence of stone boulders on the lunar surface [27]. In [28] quantitative estimates were made on the assumption that the stone boulders consist of basalt and are shaped in the form of cubes. The general conclusion drawn in [28] consists in the fact that for observations from earth the effect of the stones in the center of the lunar disk on the infrared temperature is slight. In the opinion of the author of [28] the effect of stones having dimensions from a meter to several tens of meters may turn out to be substantial in measurements made from spacecraft, since the sides that are illuminated by the sun during setting and rising and face the spacecraft may radiate ten times more energy than the remaining surface.

III. Theory of the Intrinsic Thermal Radio Emission of the Moon

1. Radio Emission from the Moon during a Periodic Surface-Heating Mode. The intrinsic radiation of a medium can be described by the equations for the transfer of radiant energy. For a dense substance (such as the lunar surface layer) this equation can be simplified using the principle of local thermodynamic equilibrium. The fact that the thickness of the layer responsible for the radiation is much smaller than the radius of the planet leads to further simplification: one can consider the planar problem. With allowance for all that has been said, the equation for radiation transfer at the frequency ν has the form

$$\cos\vartheta \frac{d}{d\tau}\left(\frac{I_\nu}{n^2}\right) = -\frac{I_\nu}{n^2} + \frac{B_\nu}{n^2}; \tag{14}$$

$$B_\nu = \mu \int I_\nu f(r) \frac{d\omega}{4\pi} + (1-\mu) n^2 B_{\nu_0}. \tag{15}$$

Here $\nu = \int_0^l \alpha_\nu dy$ is the optical thickness; α_ν is the decay coefficient, which is equal to the sum of the coefficient of true absorption ($\varkappa$) and the scattering coefficient ($\mu\alpha_\nu$), μ is a coefficient which characterizes the ratio between the scattered power and the overall amount of absorbed power; n is the refractive index of the waves in the medium; f(r) is the scattering indicatrix; ϑ is the angle between the vertical and the direction of radiation; r is the angle between the direction of radiation incident on an elementary volume and the direction of the radiation scattered by this volume; B_{ν_0} is the radiation function of the medium. In the case given this is the Planck function for the radiation flux from a medium in a vacuum.

If the medium is fairly homogeneous with depth in the thermal and electrical properties, then the solution of the transfer equation may be represented as

$$I_\nu = (1-R) \int_0^\infty B_\nu e^{-\tau \sec\vartheta} \sec\vartheta \, d\tau, \tag{16}$$

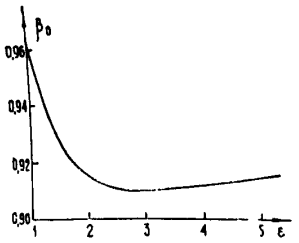

Fig. 4

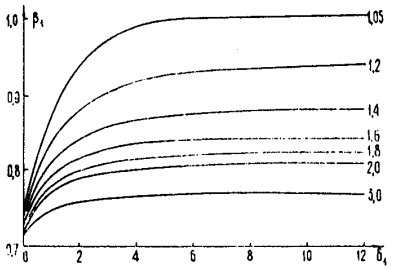

Fig. 5

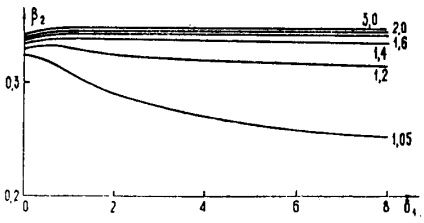

Fig. 6

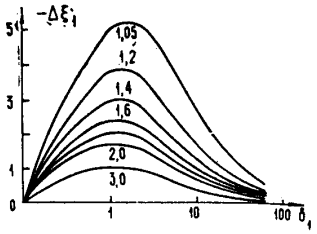

Fig. 7

where R is the coefficient of reflection of radiation from the interface boundary. If the interface surface is sufficiently smooth, then the Fresnel formulas are valid for R; for a very rough surface R should be understood to represent the albedo of the surface. However, if the medium is substantially inhomogeneous (for the given wavelength), then Eq. (16) is complicated [29], since the value of R in this case depends on the optical depth τ and is determined by the Riccati differential equation [30]. Therefore, the transmission coefficient of the radiation through the surface (1−R) must be placed in the integrand. The function B_ν in (16) is an unknown function that is defined as the solution of Eq. (15).

The entire theory of lunar radio emission has heretofore been constructed on the assumption that $\mu = 0$ for radio waves. Evidently this is valid with sufficient accuracy for waves longer than a millimeter. For waves shorter than a millimeter the scattering in the lunar substance may turn out to be substantial. Thus, if $\mu = 0$, then $\alpha_\nu = \varkappa$, while $B_\nu = n^2 B_{\nu_0}$ is a known function, and the solution for the radio range (i.e., for $h_\nu \ll kT$) is simplified considerably [12, 72]:

$$T_e(0, t, \varphi, \psi) = [1 - R(\varphi, \psi)] \int_0^\infty T(y, \varphi, \psi, t) \varkappa \sec\vartheta' e \exp(-\varkappa y \sec\vartheta') dy, \qquad (17)$$

where T_e is the effective radiation temperature of the surface elements having the coordinates φ and ψ; ϑ' is the angle at which the radiation is incident from below onto the interface; and $T(y, \varphi, \psi, t)$ is the true temperature of the lunar substance at the depth y at time t, as obtained in the form (6) as the solution of the thermal conductivity equation (1) with the boundary condition (4).

After substitution of this depth distribution of the temperature into (17), the following expression is obtained for the effective temperature of the surface elements [2]:

$$T_e(\varphi, \psi, t) = [1 - R(\varphi, \psi)] \left\{ T_0(\psi) + \sum_{n=1}^{\infty} (-1)^n \frac{T_n(\psi)}{\sqrt{1 + 2\delta_n \cos\vartheta' + 2\delta_n^2 \cos^2\vartheta'}} \cos[n\Omega t - n\varphi - \varphi_n - \xi_n(\varphi, \psi)] \right\}, \qquad (18)$$

where $\delta = \sqrt{n\Omega\rho c/2k}/\varkappa$ is the ratio between the penetration depth $l_E = 1/\varkappa$ of the electrodynamic waves and the penetration depth l_{nT} of the n-th harmonic of the thermal wave. For sufficiently small values of the loss-angle tangent the absorption coefficient is equal to $\varkappa = 4\pi\sigma'/c'\sqrt{\varepsilon}$, where σ' is the conductivity, c' is the velocity of light. Then the expression for δ takes the form

$$\delta = \frac{c\gamma\lambda}{2\pi b\sqrt{\varepsilon}} \sqrt{\frac{\Omega}{2}},$$

where $b = \tan\Delta/\rho$ is the specific loss angle tangent; $\xi_n = \arctan[\delta_n \cos\vartheta'/(1 + \delta_n \cos\vartheta')]$ is the phase shift for the n-th harmonic of the effective temperature relative to the phase of the surface temperature.

In experimental investigations of the moon in the case when the width of the radiation pattern of the receiving antenna at the 0.5 power level exceeds the angular dimensions of the moon, reception of the integral radio emission is achieved. Therefore, for a correct interpretation of the results of the measurements it is necessary to compare them with the expression for the integral radiation of the moon obtained in the exact solution. In [31] the theory of integral radio emission is given on the assumption of the homogeneity of the properties of the upper layer of the moon.

The effective temperature averaged over the disk is equal to

$$\overline{T}_e = \frac{1}{\pi}\int_{-\pi/2}^{+\pi/2}\int_{-\pi/2}^{+\pi/2}[1-R(\varphi,\psi)]\,T_e(\varphi,\psi,t)\cos^2\psi\cos\varphi\,d\varphi\,d\psi, \tag{19}$$

in accordance with [12]. Since the principal contribution to the radiation is made by the central portions of the disk, it is expedient to express the radio temperature averaged over the disk in terms of the radiation from the center of the disk by introducing the appropriate scaling coefficients. As a result, the following expression is obtained for the effective temperature of the integral radio emission:

$$\overline{T}_e = (1-R_\perp)\beta_0 T_0(0) + (1-R_\perp)\sum_{n=1}^{\infty}(-1)^{a_n}\frac{T_n(0)\beta_n}{\sqrt{1+2\delta_n+2\delta_n^2}}\cos(n\Omega t - \varphi_n - \xi_n + \Delta\xi_n), \tag{20}$$

where β_0 and β_n are the corresponding averaging coefficients; $\Delta\xi_n$ is the additional phase shift that develops during averaging.

The quantities β_0, β_n and $\Delta\xi_n$ are expressed in a very complicated way in terms of integrals that depend on ε and δ of the lunar surface. Their calculation was carried out on an electronic computer for a wide range of variation of ε and δ. Figure 4 displays the dependence of the coefficient β_0 on ε. Figures 5 and 6 display the coefficients β_1 and β_2 as a function of δ_1 for various values of ε. Figure 7 displays the dependence of the initial phase shift $\Delta\xi_1$ on δ_1 for the first harmonic. For variation of ε over wide limits the maximum magnitude of $\Delta\xi_1$ does not exceed $-5°$. An analogous phase shift for the second harmonic of the integral radiation is practically absent.

It turned out that the higher harmonics of the effective temperature averaged over the disk are substantially weakened in comparison with the corresponding harmonics of the effective temperature at the center of the disk. This means that the fluctuation of the radio temperature averaged over the disk can be described sufficiently well by just the first harmonic, which is substantiated by the results of measurements of the integral radio emission of the moon at different wavelengths; i.e.,

$$\overline{T}_e = \overline{T}_{e0} + \overline{T}_{e1}\cos(\Omega t - \overline{\xi}_1). \tag{21}$$

For comparison with experimental findings use can be made of the quantity $\overline{M}(\lambda) = \overline{T}_{e0}/\overline{T}_{e1}$ from which, evidently, as well as from (20), we have the following:

$$\overline{M}(\lambda) = \frac{T_0(0)\beta_0}{T_1(0)\beta_1}\sqrt{1+2\delta_1+2\delta_1^2}. \tag{22}$$

2. The Spectrum of the Constant Component of the Integral Radio Emission from the Moon. Exact measurements according to the "artificial moon" method revealed an increase in the constant component of the integral radio emission with increasing wavelength (see (Fig. 21), so that T_{e0} in Eq. (21) should be treated as a function of λ. As has already been indicated in §II.2 of the present review, the growth of the constant component of the radio temperature in the range of wavelengths from infrared wavelengths to $\lambda \simeq (2\text{-}3)$ cm is caused by the weak dependence of the thermal conductivity on temperature.

The growth of the constant component in the range of wavelengths $\lambda > 3$ cm was explained by the presence of thermal flux from the interior depths of the moon. In [32] the calculation is given for the constant component of the radio emission from a homogeneous lunar surface layer in the presence of heat flux from the interior. In [33, 34] estimates are obtained for the heat-flux density according to the "artificial moon" method; this flux density turns out to be close to the heat flux density at the earth. Further measurements showed that the radio-emission temperature ceases to increase at wavelengths longer than 25 to 30 cm, which is evidently evidence of the fact that there is a considerable increase in the density of the substance at depths corresponding to the penetration depth of these waves.

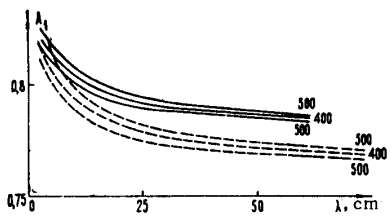

Fig. 8

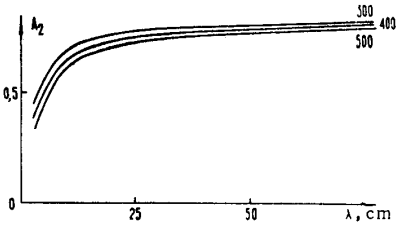

Fig. 9

Fig. 8. Dependence of the coefficient A_1 on λ for d_2 = 300; 400; 500 cm; ε = 2.25; ε_2 = 6 (solid curve) and ε_2 = 7 (dashed curves).

Fig. 9. Dependences of the coefficient A_2 on λ for d_2 = 300; 400; 500 cm; ε_1 = 2.25; ε_2 = 6.

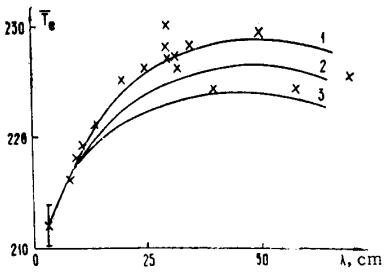

Fig. 10. Dependence of the effective temperature of the integral radio emission of the moon on wavelength for the following values of the parameters: 1. d_2 = 500 cm; $q = 0.65 \cdot 10^{-6}$ cal $\cdot$ cm$^{-2} \cdot$ sec^{-1}; 2. d_2 = 400 cm; $q = 0.72 \cdot 10^{-6}$ cal $\cdot$ cm$^{-2} \cdot$ sec^{-1}; 3. d_2 = 300 cm; $q = 0.8 \cdot 10^{-6}$ cal $\cdot$ cm$^{-2} \cdot$ sec^{-1}.

In [29] a calculation of the constant component of the integral lunar radio emission is presented in the presence of heat flux from the interior depths for an inhomogeneous model of the structure in the inside of the layer and for consideration of the temperature growth in the interior due to the temperature dependence of the thermal conductivity. For the two-layer model of the surface layer the following dependence $\overline{T}_e(\lambda)$ was obtained for $\lambda \gg hc'/kT$:

$$T_e(\lambda) = [1 - R_\perp(\lambda)]\, A_0 T_0(0) + [1 - R_\perp(\lambda)]\, qm\gamma_1 \sqrt{\frac{\tau}{\pi}}\lambda (A_1 - e^{-\varkappa_1 d_2} A_2) + [1 - R_\perp(\lambda)]\, \Delta T_{\max} \frac{2\delta_1}{1+2\delta_1} B, \qquad (23)$$

where q is the density of the heat flux from the depths of the moon; $R_\perp(\lambda)$ is the coefficient of power reflection from the lunar surface [35]; d_2 is the thickness of the porous layer; A_0, A_1, A_2, B are coefficients which appear for averaging over the disk and are complex functions of λ, d_2 and ε. The dependence of the coefficients A_1 and A_2 on wavelength λ for various values of d_2 and ε is shown, as an example, in Figs. 8, 9 while in Fig. 10 are shown the theoretical curves plotted according to (23).

3. Lunar Radio Emission during an Eclipse. The theory of radio emission from the center of the lunar disk during an eclipse is given in [18, 19]. In [19] exact and approximate expressions are obtained for the effective radio temperature of the center of the disk at each of the four time intervals t_k enumerated in §II.2. In order to compare the results with experimental data it is of interest to know the relative maximum drop $\Delta T_e(t_3)/T_{em}$, of the radio temperature, which is obviously reached at the instant t_3 corresponding to the end of the shadow phase. This value, in accordance with [19], is equal to

$$\frac{1}{M_3(\lambda)} = \frac{\Delta T_e(t_3)}{T_{em}} = -(1-R)\frac{4}{3\sqrt{\pi}}\frac{\varkappa a}{T_{em}}[\alpha_1(t_3-t_1)^{3/2} + (\alpha_2-\alpha_1)(t_3-t_2)^{3/2}]$$
$$+ (1-R)\frac{\varkappa^2 a^2}{2T_{em}}[\alpha_1(t_3-t_1)^2 + (\alpha_2-\alpha_1)(t_3-t_2)^2] \quad \left(a = \sqrt{\frac{k}{\rho c}}\right). \qquad (24)$$

As is evident from (24), the change in radio temperature is determined by the quantity $\varkappa a = 2\pi b\sqrt{\varepsilon}/c\lambda\gamma$, while in the case of lunations it depends on an analogous relationship between the electrical and thermal parameters of the substance. Actually, from Eq. (18) it is evident that the phase changes of the radio

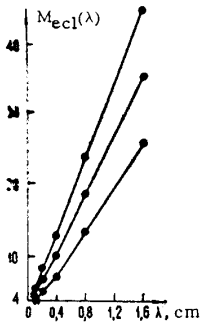

Fig. 11

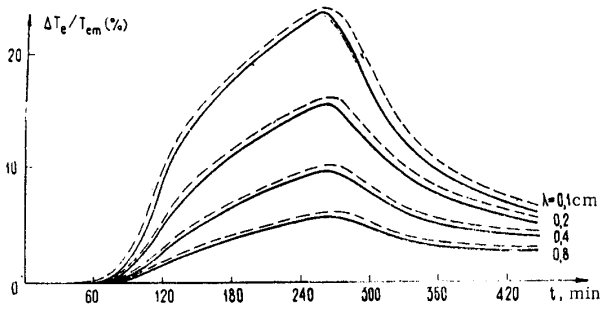

Fig. 12

temperature are proportional to the quantity $1/\delta = 2\pi b\sqrt{\varepsilon}\sqrt{2/\Omega}/c\gamma\lambda$. Thus, the reciprocal value of the change in radio temperature $M_3(\lambda)$ is theoretically an almost linear function of wavelengths λ and of the ratio between the thermal and electrical parameters. The slope of the spectrum $M_3(\lambda)$ is determined by the quantity γ/b. Theoretical curves for $M_3(\lambda)$ calculated in accordance with (24) for the circumstances of the 1963 eclipse for values of $\gamma/(b\sqrt{\varepsilon})$ equal to $7.3\cdot10^4$, $5.7\cdot10^4$, and $4.1\cdot10^4$, are shown in Fig. 11.

It should be noted that for systems used in antenna measurements the width of the directivity pattern is different, and the systems consequently produce different averaging effects. In order to clarify the applicability of the theory expounded above for the radiation from the center of the lunar disk to a description of the integral radiation [17] we performed a calculation of the integral radio emission from the moon and compared it with the radio emission from the center of the disk for the 1963 eclipse.

Figure 12 displays the relative changes of the effective temperature of the center of this disk during the eclipse at various wavelengths (the solid curves) and the corresponding changes of the effective temperature averaged over the disk (the dashed curves). The comparison shows that the maximum relative temperature drop during the eclipse, which is determined by the quantity γ/b, is practically identical in both cases. This means that in the case of the eclipse one can neglect the averaging effect of the directivity patterns of the antenna system and use the theory of radio emission for an eclipsed moon developed in [19] for the center of the lunar disk in order to determine the quantity γ/b from experimental data.

IV. The Radiative Capacity of the Lunar Surface in the Radio Range

1. The Radiative Capacity of a Smooth Surface. The radiative capacity of a flat body is assumed to be the ratio between the intensity of its radiation in the given direction and the maximum radiation on the assumption that the radiating body is absolutely black. In the case of a body having any other shape the indicated definition yields the differential radiative capacity for a flat surface element, while for the overall body it yields the integral radiative capacity. In the case of smooth surfaces that ensure specular reflection, the differential radiative capacity is simply equal to $[1-R(\varphi, \psi)]$, where $R(\varphi, \psi)$ is the Fresnel reflection coefficient for the given radiation direction. In [36] the mean-spherical radiative capacity was obtained from the constant component of the integral radio emission on the assumption that the lunar surface is smooth:

$$1 - \overline{R} = (1 - R_\perp)\alpha, \tag{25}$$

where

$$R_\perp = \left(\frac{\sqrt{\varepsilon} - 1}{\sqrt{\varepsilon} + 1}\right)^2, \tag{26}$$

ε is the dielectric constant of the substance, α is a function of ε and is given by the graph in Fig. 13.

In the general case the radiative capacity for the layer depends on the geometry of its surface (roughness) and on the variation of the dielectric properties of the substance with depth.

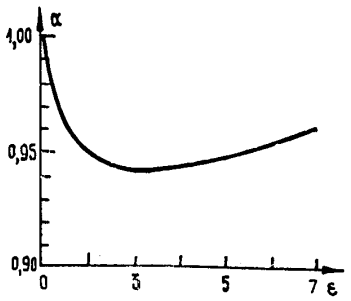

Fig. 13

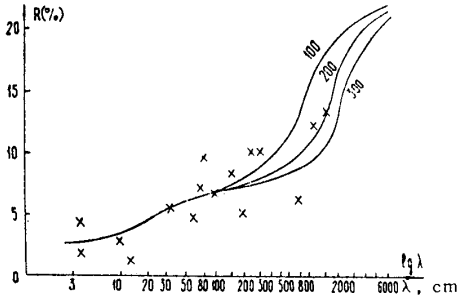

Fig. 14. Spectrum of the reflection coefficient calculated for the three-layer model of the lunar surface layer.

2. The Radiative Capacity of a Rough Surface. The actual surface of any planet has roughness. Therefore, the next approximation is in the consideration of large-scale inhomogeneities whose dimensions are considerably larger than a wavelength. The orientation of an individual area has an arbitrary slope and may be characterized by the deviation of the normal to this area from the normal to a surface that is smooth on the average. The introduction of such roughnesses leads to averaging of the radiative capacity over all values of area slopes within the limits of the attainable slope angles [12, 37]:

$$\overline{1-R(\varphi,\psi)}=\int_{-\pi/2}^{+\pi/2}\int_{-\pi/2}^{+\pi/2}[1-R(\varphi+\Delta\varphi)(\psi+\Delta\psi)]\,W(\Delta\varphi,\Delta\psi)\,d(\Delta\varphi)\,d(\Delta\psi), \tag{27}$$

where φ, ψ are the coordinates that determine the position of the area on the rough surface; $\Delta\varphi$, $\Delta\psi$ determine the deviation of the normal to this area from the normal to a surface which is smooth on the average; $W(\Delta\varphi, \Delta\psi)$ is the distribution function of the angles of deviation from the normal. In [37, 42] the calculations of the integral (27) carried out on an electronic computer are displayed for the function $W(\Delta\varphi, \Delta\psi)$ that has the form of a Gaussian curve. The calculations show that, with increasing dispersion of the slope angles, the contribution to the radiation from regions situated near the edge of the disk increases. In the central portion of the disk the radiative capacity depends very weakly on the degree of roughness of the surface.

The consideration of the surface roughnesses is necessary in determining the reflection coefficient from radar measurements, since radar methods allow the transverse back-scattering cross-section σ of the moon to be found, which in the general case may be written in the form

$$\sigma = gR_{\perp}\pi a^2, \tag{28}$$

where a is the radius of the moon; $R_{\perp}$ is the power reflection coefficient for normal incidence and is determined by Eq. (26); and g is a factor that takes into account the roughness of the surface.

Theoretically the value of g can be calculated only in two limiting cases: on the assumption that the surface of the moon is smooth (g = 1), and for the condition of purely diffuse reflection (g = 8/3). The reflection of radio waves from the surface of the moon evidently represents a certain intermediate case, and therefore the estimation of the quantity g is usually associated with a series of assumptions [104, 120]. Meanwhile it is evident from (28) that additional knowledge of the quantity g would allow the coefficient of reflection from the lunar surface to be found and consequently would allow definite conclusions to be drawn concerning the nature of the upper surface of the moon.

In [38] an attempt was made to simulate lunar back scattering in the optical range in order to explain the degree of influence of roughnesses on the factor g. For this purpose the back scattering of light by rough plates and balls was investigated. The roughness of the surface of a ball was chosen in such a way that its back-scattering pattern in the optical range coincided with the analogous pattern for the moon at the chosen wavelength in the radial range. Then the cross-section of the rough and smooth balls was measured. For a smooth ball the parameter g was assumed equal to unity. Consequently, for a rough ball $g = \sigma_k/\sigma_s$, and this quantity was assumed equal to the analogous quantity for the moon at the corresponding wavelength. The back-scattering pattern for the ball was determined from the back-scattering pattern of

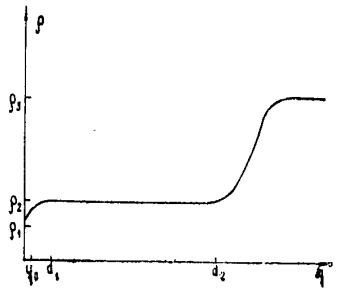

Fig. 15. Model of the density variation with depth in the lunar surface layer.

a plate made of the same material as the ball. The roughness of the surface of the two objects was created by the same means. It was found that for the moon g = 1.6 for scattering of waves in the centimeter range and g = 1.06 for scattering of decimeter waves.

3. The Radiative Capacity of a Lunar Surface Layer which is Inhomogeneous with Depth. The investigation of the intrinsic lunar radio emission indicates that the substance of the upper layer is inhomogeneous with depth. Such a structure must evidently have a complex spectrum of the power reflection coefficient. In fact, if the upper layer is less dense, then it has a lower dielectric constant. Waves incident on the surface having a wavelength much smaller than the thickness of this layer will be reflected from the upper boundary between the medium and the backing. For waves whose length is much greater than the thickness of this layer it is as if the layer did not exist, and these waves are reflected from the lower denser layers. Thus, the reflection coefficient for such a medium will vary in a certain interval of frequencies as a function of the reflection coefficient for the surface up to its value for the under layer.

As is well known, the complex coefficient of reflection from a layer having an arbitrary law for the variation of its parameters is determined by the Riccati equation [30]. In [35] the method of solving this equation on an electronic computer was used to obtain the spectrum of the coefficient of reflection from a layer whose density varies with depth according to an exponential law:

$$\rho(y) = \rho_2 - (\rho_2 - \rho_1)\exp(-y/y_0),$$

where ρ_1 and ρ_2 are respectively the densities on the surface and in the depth of the layer. At a depth y = $2.5y_0$ the density practically reaches the maximum value $\rho = \rho_2$. The following relationship between the thickness of the inhomogeneous layer and the average wavelength of the transition range is obtained:

$$l = 2.5\,y_0 = \lambda_{av}/8.$$

In [39] spectra are also presented of the reflection coefficient for certain three-layer models of the surface layer of the moon, which were found by numerical integration on an electronic computer. In the calculations the frequency dependence of the dielectric constants [40] was taken into account in accordance with (32) and (33).

In Fig. 14 is shown the spectrum of the reflection coefficient for the surface-layer model whose qualitative density variation with depth is displayed by the graph in Fig. 15. The calculation was carried out for the following values of the parameters: y_0 = 1.5 cm, $\rho_1 = 0.7\,g\cdot cm^{-3}$, $\rho_2 = 1\ g\cdot cm^{-3}$, $\rho_3 = 2.5\ g\cdot cm^{-3}$, d_2 = 100, 200, 300 cm.

4. Polarization of the Radio Emission of a Rough Surface. The magnitude of the polarization coefficient of lunar radio emission in the most general case is equal to the ratio between the difference and the sum of the effective temperatures determined for two mutually perpendicular orientations of the electric vector of the antenna averaged over the radiation pattern [12]:

$$p = \frac{\overline{T}^{\theta}_{e1} - \overline{T}^{\theta}_{e2}}{\overline{T}^{\theta}_{e1} + \overline{T}^{\theta}_{e2}}; \qquad (29)$$

$$\overline{T}_e^0 = \left\{ \int_{-\pi/2}^{+\pi/2} \int_{-\pi/2}^{+\pi/2} [\overline{R}_h(\varphi, \psi) - \overline{R}_v(\varphi, \psi)] \, [\sin^2(\gamma - \Delta) - \cos^2(\gamma - \Delta)] \, F(\varphi, \psi) T_e(\varphi, \psi, t) \right.$$

$$\left. \times \cos^2\psi \cos\varphi \, d\varphi \, d\psi \right\} \left\{ \int_{-\pi/2}^{+\pi/2} \int_{-\pi/2}^{+\pi/2} [\overline{R}_h(\varphi, \psi) + \overline{R}_v(\varphi, \psi)] F(\varphi, \psi) \cos^2\psi \cos\varphi \, d\varphi \, d\psi \right\}^{-1}, \quad (30)$$

where $\overline{R}_n(\varphi, \psi)$ and $\overline{R}_V(\varphi, \psi)$ are the mean-statistical reflection coefficients for the vertical and horizontal polarization, as determined by Eq. (27); γ is the angle between the plane of the principal meridian and the projection onto the picture plane of the radius-vector directed from the center of the moon to the point having the coordinates φ, ψ; Δ is the angle between the plane of the electric vector of the antenna and the plane of the principal meridian; $T_e(\varphi, \psi, t)$ is the effective temperature of the considered sector for the case of an absolutely black moon; $F(\varphi, \psi)$ is the radiation pattern of the receiving antenna. As is evident from Eq. (30), the polarization coefficient is determined by three quantities: the temperature distribution $T_e(\varphi, \psi, t)$; the radiation pattern $F(\varphi, \psi)$ and the radiation capacity $1 - R(\varphi, \psi)$.

In [12] an estimate was made of the polarization coefficient of the lunar radiation for the case when the lunar surface was smooth, the radiation pattern of the antenna was broad compared with the angular dimensions of the planetary disk ($F(\varphi, \psi) = \text{const}$), and $T_e(\varphi, \psi, t)$ is the sum of the constant component and first harmonic of the radio temperature. It was shown that the degree of polarization of the integral lunar radio emission is determined solely by the deviation of the temperature distribution over the disk from a centrally-symmetrical distribution and specifically by the degree of falloff of the temperature toward the lunar poles.

In [41] the problem of the polarization of the integral lunar radiation was treated on the assumption that its surface has large-scale roughnesses. The calculations that were performed showed that the magnitude of the polarization coefficient depends on the lunar phase and reaches a maximum near quadratures. With increasing wavelength the alternating component of the polarization decreases and is practically absent at the wavelength $\lambda = 3.2$ cm.

In [43-48] the problem of the averaging action of the radiation pattern for measurement of the polarization was considered. In [46] it was assumed that the radiation pattern is a body of rotation whose cross section has the shape of a Gaussian curve. The variation of the polarization coefficient along the radius of the lunar disk is shown in Fig. 16 for various values of the width θ of the radiation pattern at the half-power level. It was assumed that the lunar surface is ideally smooth. It is evident that the polarization coefficient is practically independent of the width of the radiation pattern in the central disk region bounded by a circle having the radius $0.6\,R_M$. The results of calculating p for $\varepsilon = 1.5$ and 3 and various values of the dispersion σ are shown in Fig. 17. For $r/R_M < 0.6$ the polarization coefficient is practically independent of the quantity σ. The effect of roughnesses is only manifested near the limb of the lunar disk.

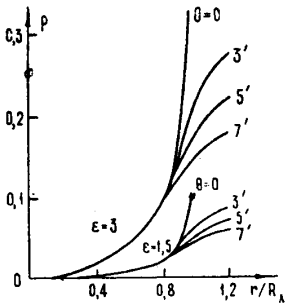

Fig. 16

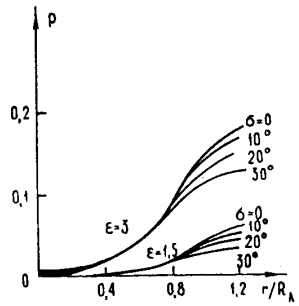

Fig. 17

Fig. 16. Variation of the polarization coefficients along the radius of the lunar disk for $\theta = 0$, 3' 5', 7' and $\varepsilon = 3$; 1.5.

Fig. 17. Variation of the polarization coefficient along the radius of the lunar disk for $\theta = 7'$, $\sigma = 0$, 10, 20, 30° and $\varepsilon = 3$; 1.5.

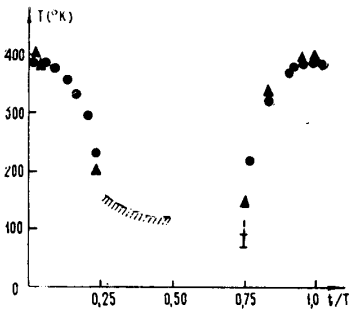

Fig. 18

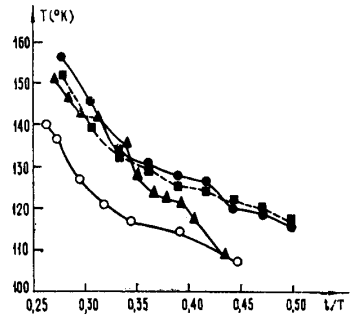

Fig. 19

Fig. 18. Variation of the surface temperature at the center of the lunar disk from the experimental data of: ▲▲▲) Sinton, et al. [49]; ●●●) Saary and Shorthill [49]; III) Low [51].

Fig. 19. Variation of the surface temperature of the center of the disk during the lunar night from the experimental data of: ●●●, ■■■) Surveyor-V [49]; ▲▲▲) Shorthill and Saary [49]; ○○○) Murray and Wildey [50].

The polarization characteristics of the lunar radio emissions for the reception of radiation by an antenna having a radiation pattern of the knife-edge type were obtained in [43-45, 47]. In [43-45] the case of roughness with a uniform distribution of the slope angles within specified limits was considered without allowance for shading, and it was assumed that the statistics of the slope angles of the roughnesses is governed by a normal law. Calculations showed that for passage of the central portion of the lunar disk through the radiation pattern a vertical polarization is observed, the polarization coefficient under these conditions being weakly dependent on σ and θ. Near the lunar limb the polarization is horizontal; here the polarization coefficient depends substantially on the width of the radiation pattern in a narrow cross section and on the dispersion of the slope angles of the roughnessses.

In [45, 48] there is an analysis of the polarization characteristics of lunar radio emission with allowance for the averaging action of the multiload radiation pattern which is formed by a two-element radio-interferometer. It is shown that measurement of the polarization coefficient by the interferometer is expediently performed for n = 1-1.5 (n is the number of lobes which fits on the lunar disk), where the effects of ε and σ are most noticeable.

Thus, the calculations that were performed show that the measurements of the polarization coefficient in the central region ($r/R_M < 0.6$) allow the dielectric constant of the lunar surface layer to be found. The effect of roughness is manifested only near the lunar limb, which provides the possibility of using the value of the polarization coefficient near the limb to estimate the degree of roughness of the lunar surface after first having determined ε.

V. The Results of Measurements of the Intrinsic Radiation from the Moon

1. The Results of Infrared Measurements. The earliest measurements of the intrinsic lunar radiation, which had important significance for the investigation of the latter, were carried out by Pettit and Nicholson [1] in the infrared range. They obtained the temperature of the subsolar point, the midnight temperature, the intensity distribution of the radiation over the disk during full-moon, and likewise the temperature variation of the area near the center of the disk and near the limb during an eclipse.

The increase in the sensitivity of the receivers in the infrared range allowed a number of observations to be carried out with a high resolution. The results of measurements of the temperature of the surface area at the lunar equator during lunations are shown in Fig. 18 [49]. In the measurements of the day temperature performed by Sinton, et al., (see, for example, [49]) a narrowband filter at $\lambda = 8.8\ \mu$ was used. Maps of the isotherm of the illuminated surface were obtained for nine phase angles having a resolution of 25 seconds of arc (1 second of arc is of the order of 1/1800 lunar diameters). The day temperature

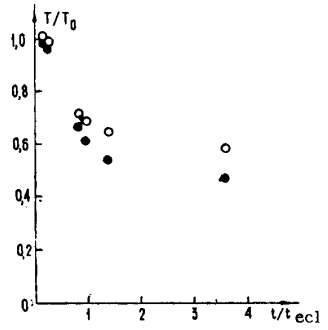

Fig. 20. Variation of the surface temperature during the eclipse of December 19, 1964 according to the experimental data on: ○○○) the Tycho crater; ●●●) the region in the neighborhood of the Tycho crater.

was likewise measured by Saary and Shorthill [49] with a high resolution equalling 1 second of arc. The measurements were carried out in the range of wavelengths $\lambda = 10\text{-}12\ \mu$ at 23 values of the phase angles.

The temperature of the lunar surface after the setting of the sun has been less adequately studied, since for these measurements more sensitive instruments are required. The hatched region in Fig. 18 is represented in greater detail in Fig. 19. The measurements performed by Murray and Wildey [50] were carried out in the interval of wavelengths $\lambda = 8\text{-}13\ \mu$ with a resolution of 26 seconds of arc. The extrapolation of these results to time $t/T = 0.5$ yields the estimate for the midnight temperature of the lunar surface $T_N \sim 104°$. The data obtained by Surveyor-V [49] were treated as the upper possible boundary of the night temperature. However, in [130] it was shown that a more thorough analysis of these results with allowance for all possible measurement errors allowed elimination of the difference between the Surveyor-V data and the results of terrestrial measurements. Measurements just before sunrise were performed by Low [51] at a wavelength $\lambda = 17.5\ \mu$. It turned out that the average surface temperature was equal to 90°, although there were regions having a temperature lower than 70°.

Interesting results were obtained in measuring the cooling of the lunar surface during the eclipse of September 19, 1964. The measurements were carried out by two groups: Saary and Shorthill [52] and Ingrao, Yang, and Linsky [26]. The results of the second group are shown in Fig. 20. The filled circles describe the cooling of regions that are 30 seconds of arc to the east and west of the crater Tycho; the open circles describe the cooling of the region inside the crater Tycho. From Fig. 20 it is evident that the cooling of the inside of the crater observed during the lunar eclipse is slower than the cooling of the surrounding areas. On the photographs of the eclipsed moon in infrared rays such craters appear as being extremely light; in the literature they have been called "hot spots." At present 330 anomalously light regions have been revealed. They have been classified for the purpose of establishing a relationship to the visual features of the lunar contour. The results of this classification have shown that approximately 90% of all "hot spots" are associated with craters and turn out to be lighter during the full-moon as well. Approximately 10% of the spots are not associated with any contour features.

The following possible explanations of the observed phenomenon are discussed in the literature.

1. Different emission capacities of individual areas on the lunar surface [53]. However, as estimates show, in order to ensure the necessary temperature difference in tens of degrees, the emission capacities of the areas must differ by a factor of two.
2. A different transparency of the substance of the areas in the infrared range [54]. But evidently the objections to this are the same as to the previous hypothesis: differences in the transparency within individual areas are required which are too great.
3. The existence of internal sources of heat. The objection to this hypothesis is the fact that the anomalous regions frequently do not appear to be warmer during the lunar day.
4. Scattering by the rough surface. A surface covered with roughnesses of the order of several centimeters will appear to be warmer than a flat surface consisting of the same rocks [23, 55].
5. The emergence of harder rocks onto the surface [53]. Such a structure must generate thermal anomalies and would appear to be more probable. However, as calculations [21] show, the temperature of the "hot spots" in the case of purely hard-rock surfaces must be substantially higher than that observed.

TABLE 1

No.	λ (cm)	T_{e0}(°K)	T_{e1}(°K)	ξ_1 (deg)	Measurement error (± %)	Radiation pattern half-width	Authors
1	2	3	4	5	6	7	8
1	0,087	191	140	5	15	11	Fedoseev et al. [131]
2	0,106	179	117	15	12	13,5	" [131]
3	0,126	179	119,5	5	12	8	" [131]
4	0,13	219	120	16	15	10	Fedoseev [85]
5	0,145	189	110	2	15	18,5	Kukin, Fedoseev [131]
6	0,18	240	115	14	20	6	Naumov [84]
7	0,225	201	80	18	10	10	Kislyakov, Naumov (in press)
8	0,40	230	73	24	10	25	Kislyakov [79]
9	0,40	228	85	27	15	1,6	Kislyakov, Salomonovich [91]
10	0,40	204	56	23	4	36	Kislyakov, Plechkov [132]
11	0,8	197	32	40	10	18	Salomonovich [76]
12	0,8	211	40	30	15	2	Salomonovich, Losovskii [89]
13	0,86	180	35	35	15	12	Gibson [94]
14	1,25	215	36	45	10	45	Piddington, Minnet [72]
15	1,25	222	40	64	5	40	Plechkov [100]
16	1,45	215	36	37	5	40	Plechkov [100]
17	1,63	208	37	30	3	44	Kamenskaya et al. [99]
18	1,63	207	32	10	3	44	Dmitrenko et al. [66]
19	1,8	202	24	30	5	63	Plechkov [100]
20	2,0	206	19	56	5	60	Plechkov [100]
21	2,0	190	20	40	7,5	4	Salomonovich, Koshchenko [88]
22	2,5	210	15,5	42	5	72	Plechkov [100]
23	3,15	195	12	44	15	9	Mayer et al. [24]
24	3,2	223	17	45	15	6	Koshchenko et al. [87]
25	3,2	245	16	41	15	40	Strezheva, Troitskii [80]
26	3,2	210	13,5	55	2,5	72	Kroitkov et al. [57]
27	3,2	213	14	26	2	87	Bondar et al. [60]
28	3,2	216	16	15	3	40	" [60]
29	7,93	216	7	45	3,5	73	Alekseev et al. [69]
30	9,4	220	5,5		5	140	Medd, Broten [81]
31	9,6	218	7	40	2,5	100	Krotikov [62]
32	11	214			12	17	Messger, Strassl [56]
33	11	219	6	55	3	110	Alekseev et al. [69]
34	14,2	221	—	—	2,5	140	" " [69]
35	20,8	225	—	—	2,5	200	" " [69]
36	20,8	205	5	36			Waak [133]
37	21	217	5,3	48	2	36	" [133]
38	21	250	5		15	35	Messger, Strassl [56]
39	23	254	6,5		15	38	Castelli et al. [97]
40	25	226	—	—	3	180	Alekseev et al. [71]
41	30,2	227	—	—	3,5	210	" " [71]
42	32,3	233	—	—	2,5	180	Razin, Fedorov [86]
43	35	236	—	—	4	186	Krotikov et al. [64]
44	36	237	—	—	3	190	" " [64]
45	40	224	—	—	5	40	" " [64]
46	50	229	—	—	3	280	" [65]
47	58	224	—	—	—	—	Troitskii et al. [83]
48	70,16	225	—	—	3,5	90	Krotikov et al. [68]
49	168	233			4	13,6·4°	Baldwin [134]

2. The Method of Exact Measurements of Lunar Radio Emission ("Artificial moon" method). The effective temperature $\overline{T}_e$ of lunar radio emission is proportional to the signal power at the antenna output and is measured by means of radiometers. The proportionality coefficient is determined by the antenna parameters (directivity, losses in the antenna path, the radiation pattern). The difficulty in determining the parameters indicated leads to considerable measurement errors. The accuracy of determining $\overline{T}_e$ by this direct method usually does not exceed 10 to 20%, which severely restricts the possibility of using radio data for determining the physical parameters of the lunar surface layer.

The majority of experimental results on the intrinsic lunar radio emission that are given below were obtained by the exact "artificial moon" method [57]. This method is based on comparing the lunar radio emission with the known radio emission from an absolutely black disk situated in the Fraunhofer zone of the antenna (distance from the telescope $R \geq D^2/\lambda$, where D is the diameter of the mirror, λ is the wavelength) at a sufficient angle of elevation against the background of the sky. The signal power from the disk is proportional to the known quantity

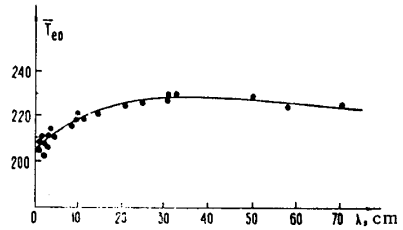

Fig. 21. Experimental spectrum of the constant component of the integral radio emission.

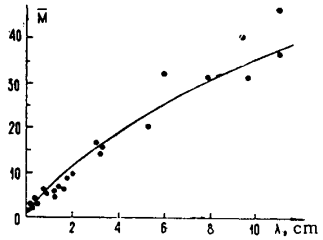

Fig. 22. Experimental spectrum of $\bar{M} = \bar{T}_{e0}(\lambda) / \bar{T}_{e1}(\lambda)$.

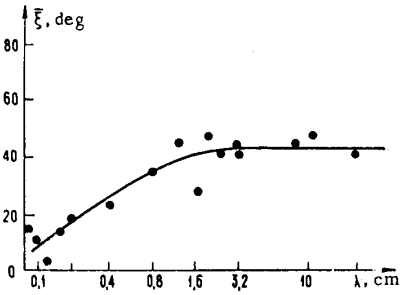

Fig. 23. Experimental spectrum of the delay of the first-harmonic phase.

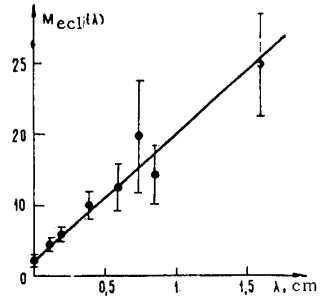

Fig. 24. Experimental spectrum of $\bar{M}_{ed} = \bar{T}_{em} / \Delta\bar{T}_e$.

$$T_d \int_{\Omega_d} F d\Omega,$$

where T_d is the disk temperature, which is equal to the temperature of the surrounding air; F is the radiation pattern of the antenna; Ω_d are the angular dimensions of the disk that are visible from the aperture of the antennas. Making use of this value, it is easy to calibrate the entire system without resort to measurement of the power at the antenna output and using only the precisely known parameters of the antenna.

It turned out that the most substantial error of the method is associated with the effect of the earth's radio emission and the nonuniform radiation from the sky which is diffracted by the disk and is incident in the radio telescope, thus increasing the standard signal by an indeterminate amount. In [57] it was shown that the use of two additional screens – a black disk and an aperture in a black plane (the diameter of the aperture is exactly equal to the disk diameter) – allows the diffraction error to be eliminated. Due to the use of the second standard the conditions for placing the disk were found for which the influence of the earth's radio emission may be reduced to the minimal possible magnitude.

In [58, 59] a calculation of the correction due to diffraction of the earth's radiation and the background by the disk was carried out. All of this allowed just the standard disk to be used for subsequent measurements of the lunar radio emission. The "artificial moon" method made possible the determination of the temperature of the integral lunar radio emission with an accuracy of 2 to 3% over a wide range of wavelengths.

3. Experimental Data on Lunar Radio Emission during Lunations and during Eclipses. Heretofore extensive experimental material has been accumulated on the intrinsic lunar radio emission during lunations over a wide range of wavelengths from 0.7 mm to 150 cm. The results of these measurements are presented in Table 1.

As is evident from Eq. (21), the intrinsic lunar radio emission is conveniently characterized by the spectra of three quantities: a constant component, the first-harmonic amplitude, and the delay of the phase

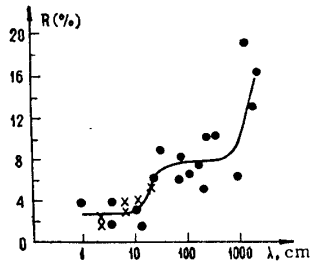

Fig. 25. Experimental spectrum of the reflection coefficient.

of the radio temperature relative to the optical phase. The spectrum of the constant component of the integral radio emission, which has basically been obtained by the method of exact measurements using an "artificial moon" [32, 57, 60-62, 64-71, 75-80, 82-86], is displayed in Fig. 21. The spectrum of the first-harmonic amplitude, which is characterized by the ratio $\bar{M}(\lambda) = \bar{T}_{e0}(\lambda)/\bar{T}_{e1}(\lambda)$, is displayed in Fig. 22 [2, 57, 60-92], from which it is evident that at wavelengths longer than 15 to 20 cm the fluctuations of radiation intensity practically vanish. The spectrum of the phase delay of the first harmonic $\bar{\xi}_1(\lambda)$ is shown in Fig. 23 [2, 57, 60-92].

Important information on the properties of the substance forming the upper layer is incorporated in the data on the variation of the radiation intensity during lunar eclipses [1, 18-20, 95-100]. These data are presented in Fig. 24 where the ordinate shows the quantity $\bar{M}_{ed} = \bar{T}_{em}/\Delta\bar{T}_e$, equal to the reciprocal of the maximum relative intensity falloff that is characteristic of the end of the shadow phase of the eclipse of the center of the lunar disk. As is evident from Fig. 24, there is practically no variation of the intensity during the eclipse at wavelengths longer than 1.5 cm.

VI. Results of Measuring the Spectrum of the Reflection Coefficient

A fairly essential characteristic of the lunar surface layer is the spectrum of the reflection coefficient. The values of the reflection coefficient over a wide range of wavelengths were obtained both by radioastronomy methods and by radar methods. Several radioastronomy methods were used to determine the reflection coefficient – for example, from the constant component of the radio temperature [36], from the polarization of the intrinsic radiation [102, 43-48], and from the distribution of the brightness temperature over the disk [37, 89, 101]. But the principal contribution to the results of investigating the spectrum of the reflection coefficient is made by radar measurements carried out over a wide range of wavelengths [103-109]. The filled circles in Fig. 25 denote the values of the coefficient of radar reflection, reduced in accordance with the values of g indicated in §IV.1 of the present review. The same figure shows crosses representing the data obtained on the basis of measuring the polarization of the radio emission.

VII. Laboratory Investigations of Earth Rocks

The natural assumption of the identity of rocks making up the upper layers of the moon and the earth has led to numerous laboratory investigations of earth rocks. In the optical range of wavelengths a comparison was made with respect to such characteristics as brightness, color, albedo, scattering indicatrix, back-scattering curves, reflected-light polarization, and the shape of the reflection capacity as a function of the spectrum. Barbashev and Chekirda obtained extensive experimental material [110], on the basis of which they concluded that the lunar surface is evidently covered with tuff-like rocks in a highly crumbled state with grain dimensions of 3 to 10 mm. In [111] the albedo and back-scattering curves were measured for 200 different surfaces: mountainous, metallic, natural (grass, lichen, moss), artificial (wire wound on a flat surface, etc). A comparison with the lunar curves for back-scattering allowed the authors to conclude that the lunar surface is covered with mountain dust having grain dimensions of 10 to 15 μ, which forms a complex porous structure under conditions of the lunar vacuum. The lower albedo of lunar rocks in comparison with that of earth rocks was explained by Hapke [112] on the basis of bombardment with fast

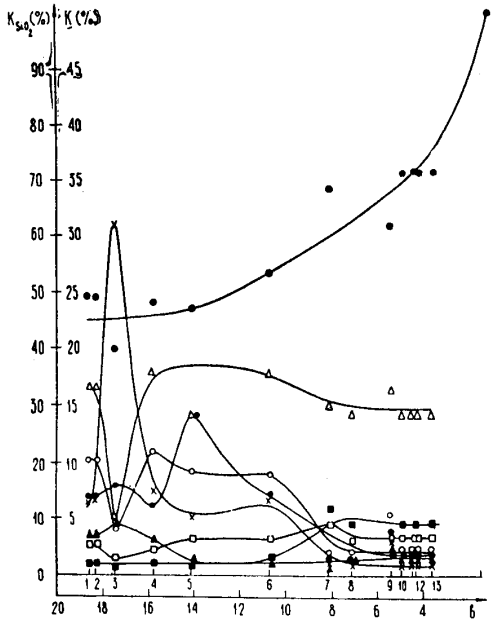

Fig. 26. Variational diagrams of the losses of eruptive intrusive rocks. 1) Gabbro–diabase No. 1; 2) gabbro–diabase No. 2; 3) periodotite; 4) gabbro No. 1; 5) gabbro–diabase No. 3; 6) gabbro No. 2; 7) granite–applite; 8) granite No. 1; 9) quartz diorite; 10) granite No. 2; 11) granite No. 3; 12) intermediate-grain granite; 13) granite No. 4. The dependence of the specific loss-angle tangent on the percentage content in the rocks for: ●●●) SiO_2; ΔΔΔ) Al_2O_3, etc.

particles. Thorough measurements of the polarization of light reflected by the moon and various earth rocks were carried out by Lyot [113] and later by Dollfus [114], which allowed them to conclude that the lunar surface is probably covered with a thin layer of volcanic dust or ash.

However, all of the optical comparison methods enumerated above yield information only on the thin surface layer whose properties may differ from the properties of deeper layers. Moreover, the methods indicated do not allow determination of the chemical nature of the substance. Actually, such characteristics as scattering and polarization of light as a result of reflection depend basically on the surface geometry (the character of the roughnesses) rather than on the composition. Thus, in [111] it was found that the lunar curves are satisfied by the curves for back scattering from the surface of lichen having a porous structure. Evidently, the only possibility for determining the chemical composition of the substance forming the upper layer of the moon from earth is a comparison of the electrical characteristics of the lunar surface with the corresponding characteristics of earth rocks. The method of estimating the chemical substance of the moon from radioastronomy data is based on the assumption that the solid substance of the moon is a composition of silicate rocks, just as it is on earth.

Measurements of the loss-angle tangent $\tan\Delta$ and the dielectric constant ε of various rocks showed that these quantities depend very strongly on chemical composition and therefore may serve to determine it. However, as is well known, the parameters $\tan\Delta$ and ε depend not only on the chemical composition but also on the density of the rock. In this connection it was noted in [16] that for comparison purposes it is necessary to make use of certain functions of $\tan\Delta$ and ε that would not depend on the density of the substance (i.e., would be density-invariant). Theoretical and extensive experimental investigations of eruptive rocks [115] showed that with sufficient accuracy $\tan\Delta/\rho = b$ and

$$(\sqrt{\varepsilon} - 1)/\rho = a \qquad (31)$$

do not depend on the density ρ over a wide range of density variation. The measurements allowed detection of a fairly sharp dependence of $b = \tan\Delta/\rho$ on the amount of the oxide SiO_2 in the rocks.

The dependence obtained served for estimates of the SiO_2 content in the lunar substance, which was found to equal 55 to 65% by weight [115-118]. Special experimental investigations of mountain rocks carried out in the 30 to 500 MHz range [40] showed that the quantities b and a are essentially determined by the chemical composition of the rocks and partially by the form of the crystalline structure (i.e., by the history of formation of the rocks – intrusive, effusive). It turned out that the quantity b for rocks ranging from

acidic to basic varies by more than a factor of 20, while the quantity a varies by a factor of 2.5 from 0.25 for acid rocks to 1.1 for ultrabasic rocks. The quantity b is practically independent of frequency in the centimeter and decimeter ranges, whereas a reveals a noticeable frequency dependence. The frequency dependence averaged over all rocks may be represented by the following empirical formula:

$$a(\lambda) = a_0 + \xi \lg \lambda/\lambda_0. \tag{32}$$

As measurements of various earth rocks at a wavelength $\lambda_0 = 3$ cm showed [115], the average value over all rocks is $a_0 = 0.5$. Consequently, Eq. (31) takes the form

$$a(\lambda) = 0.5 + 0.045 \lg \lambda/3. \tag{33}$$

An analysis of the values of b and a obtained [40] showed that a definite dependence of these quantities on the concentration of some oxide in the rocks can be traced. It is most expedient to display this dependence in a form analogous to a Harker variational diagram [118]. The quantity a or b is represented on the abscissa for some rocks, while the values of oxide content in the rocks are represented on the ordinate. As a result, for certain intrusive rocks the diagram in Fig. 26 was obtained [119], the data on the chemical composition of the rocks being taken basically from typical analyses known from the literature for the type of rock considered during the construction of the diagram.

The presence of a regular relationship between the parameters b and a and the chemical composition is related to the fact that the variations of the composition are not arbitrary in the rocks. Silicate rocks having an arbitrary content of various oxides do not exist (for example, the reduction of SiO_2 content in going over from one rock to another leads on the average to definite changes in the content of one or several other oxides). Actually this means that, for example, the percentage composition of SiO_2 in a rock on the average determines the content of the remaining oxide and consequently the type of rock.

Recently measurements were carried out of the dielectric constant and loss-angle tangent of a number of mountain rocks at frequencies of 35 and 450 GHz [128]. The resulting data are in good agreement with the propositions stated above concerning the dependence of the electrical properties on the chemical composition of the substance and on frequency.

VIII. Interpretation of the Data on Intrinsic and Reflected Radiation, and on the Structure and Properties of the Substance of the Upper Layer of the Moon

Let us now briefly consider methods of interpreting experimental data on the intrinsic radiation and the reflection of radio waves for the purpose of obtaining information on the properties and structure of the substance making up the upper layer of the moon. Under these conditions we shall not give a detailed exposition of the calculations carried out in the corresponding papers but shall restrict ourselves to a description of the physical essence of the analysis.

The ensemble of equations (1)-(3), (14), (15) completely determines the intrinsic radiation of the moon. Consequently, the various characteristics of the radiation may be used (at least, in principle) to determine all of the parameters of the substance that are included in the equations. For this purpose we usually seek the solution for a family of parameter values that are then determined by comparing calculation with experiment. In practice this is possible when the solution depends on only one parameter. However, we have about ten unknown parameters (k, c, ρ, ε, d, q, etc.) and, furthermore, the majority of them are in the general case functions of depth and sometimes even functions of temperature. Therefore, the method of analysis must consist in choosing from the radiation characteristics those that are principally determined by one parameter; the other parameters either have no effect at all on them or affect them so slightly that this phenomenon may be neglected in the first approximation.

After such a choice has been made on the basis of the theoretical analysis, the observed phenomenon is used to determine some parameter (i.e., in order to explain the radiation character of the disk or a group of characteristics, the appropriate particular model is constructed). The collection of partial models which explains the entire available experimental material allows the creation of an overall model that best satisfies all of the data. Just such an approach was used in studying the moon. Let us now consider the specific interpretive results.

TABLE 2

Element	Surveyor-V	Surveyor-VI	Surveyor-VII	Radioastronomy
O	58±5	57±5	58±5	62±4
Si	18,5±3	22±4	18±4	20±1
Al	6,5±2	6,5±2	9±3	7±0,5
Mg	3±3	3±3	4±3	2±1
Fe, Ca	13±3	5±2, 6±2	2±1, 6±1	2±0,5, 2±1
K	—	—	—	1,5±0,5
Na	2	2	3	1,5±0,5

1. The Quasihomogeneity of the Properties of the Substance with Depth. The possibility of detecting abrupt inhomogeneities of the surface layer with depth is associated with the variable thermal mode and with the fact that the data of intensity measurements at various wavelengths correspond to measurement of the temperature at different depths. With increasing wavelength of the received radiation the study proceeds as if it were depth sounding of the layer. Any abrupt changes in the properties of the upper layer with depth lead to a change in the temperature distribution and may consequently be detected in the spectrum of the radio emission. Because considerable temperature gradients develop due to the solar flux in the upper layer having a thickness (3-4)l_T, this layer appears to be the most accessible for study. (The spectra of the first-harmonic amplitude and the delay phase, for example, carry information only on this layer having a thickness of the order of several tens of centimeters.) But, as we shall see below, due to the considerable heat flux from the interior of the moon and the low thermal conductivity of the substance making up the upper layer, it turns out to be possible to investigate the surface layer down to considerable depths.

An analysis of the amplitude spectrum of the first harmonic of the radio temperature (Fig. 22) showed that it satisfies the homogeneous surface-layer model well and does not correspond at all to the abruptly-inhomogeneous model that assumes the existence of a dust layer having a thickness of several millimeters covering dense rocks [16]. The spectrum of the delay of the phase of the first harmonic $\xi_1(\lambda)$ (Fig. 23) also is evidence of an approximately homogeneous distribution of the thermal properties of the substance with depth. The limiting phase delay for increasing λ is equal to 45°. It is precisely this value that is obtained in the theory of the homogeneous model [12]. Any significant inhomogeneity, especially of the dust layer, leads to a noticeable increase in the limiting delay [72]. Thus, the quasihomogeneous model of the uppermost layer is in fairly good agreement with the spectrum of the intrinsic radiation.

2. The Thermal Parameter γ. As was said in §II.1 of the given review, for calculation of the thermal mode of the surface the validity of the homogeneous model in which the properties do not depend on temperature and do not vary with depth was assumed in the first approximation. In the second approximation the homogeneous model with thermal conductivity and specific heat that are dependent on temperature was considered.

From the measurements it is at present known sufficiently accurately that the midnight surface temperature $T_N = 100°K$, the midday temperature $T_D = 395°K$, the ratio between the constant component and the amplitude of the first harmonic of the integral radiation at $\lambda = 0$ (i.e., in the infrared range) is $T_0/T_1 = 1.3$ (see Fig. 22), while the relative temperature drop during an eclipse (in the same range) is $\Delta T_e/T_{em} = 0.52$ (see Fig. 24). The comparison of these quantities with the results of the theoretical computation of the thermal surface mode in the homogeneous-model approximation with allowance for the dependence of the thermal conductivity and specific heat on temperature [11] leads to the following values of the parameter γ:

$$\gamma_1(300°K) = 1000 \text{ cal}^{-1} \cdot \text{cm}^2 \cdot \text{sec}^{1/2} \cdot \text{deg},$$

$$\gamma_2(300°K) = 800 \text{ cal}^{-1} \cdot \text{cm}^2 \cdot \text{sec}^{1/2} \cdot \text{deg},$$

for eclipses and lunations, respectively.

The eclipse values of γ refer to the uppermost layer, while the lunation values refer to a layer which is ten times thicker. The closeness of the values of γ for the eclipse and lunation processes likewise substantiates the approximate homogeneity of the properties with depth.

3. The Parameter $\delta = l_E/l_T$. The penetration depth $l_E = 1/\varkappa_\nu$ of the electrical wave characterizes the effective thickness of the radiating layer. It is evident that the greater the depth l_E of the radiating layer in comparison with the penetration depth l_T of the thermal wave, the smaller the amplitude of the intensity oscillations. Consequently, the spectrum $\bar{M}(\lambda)$ characterizes the magnitude of the ratio $\delta = l_E/l_T$.

A comparison of the experimental spectrum $\bar{M}(\lambda)$ with the corresponding theoretical dependence $\bar{M}_{theor}(\lambda)$ stipulated by Eq. (22) leads to the value $\delta \simeq 2.3\lambda$. The spectrum obtained for the quantity $l_E = 2.3 l_T \lambda$, just as in the case of the first-approximation model ($l_\nu = 2 l_T \lambda$), indicates the dielectric nature of the matter making up the upper layer of the moon. It is most probable that such a dielectric may consist of rocks analogous to terrestrial rocks (i.e., silicates). This immediately yields a value of specific heat that is equal to $c(300) = 0.19$ cal $\cdot g^{-1} \cdot deg^{-1}$ for all silicates (with an accuracy of up to 10%) at T = 300°K.

4. The Density of the Substance Making up the Lunar Surface Layer. Expression (31) presented above establishes the actual relationship between the dielectric constant of the substance and its density. Therefore all possible methods of measuring ε that are described below in §VIII.6 of the review allow the density of the substance making up the upper layer to be determined. Data are available that indicate a certain weak inhomogeneity of the dielectric properties of the substance with depth in the upper layer of the order of several centimeters. This does not contradict the statement made above that the spectra of the amplitude and of the delay phase correspond to the homogeneous model. The weak inhomogeneity for which the properties of the substance vary with depth insignificantly and smoothly (by a factor of 1.2-1.3 in density) is shown by the calculations to have little effect on the character of these spectra. In this case their variations lie within the limits of the accuracy of the measurements.

In order to reveal the inhomogeneity it is necessary to find those radiation parameters that are sensitive to it. Such parameters are the reflection coefficient of radio waves, the polarization of the radiation, and the value of the eclipse and night temperatures of the surface. An increase in the reflection coefficient in the range of wavelengths from 15 to 30 cm (see Fig. 25) may merely indicate an actual frequency dependence of the dielectric constant of the substance, or the existence of inhomogeneity of the dielectric properties as a function of depth. The first proposition is not correct, since an increase in ε with wavelength according to the Kramers–Kronig theorem would unavoidably lead to an increase of the losses in this range of wavelengths and this would affect the spectrum of $\bar{M}(\lambda)$. As yet this has not been revealed. Evidently the second case holds.

As was shown in §IV.3 of the present review, the calculation of the reflection coefficient for an exponential variation of the density with depth shows that the wavelength λ_1 near which the change in reflection coefficient occurs is related to the characteristic dimensions y_0 of the layer by:

$$20 y_0 = \lambda_1.$$

From experiment (see Fig. 25) $\lambda_1 = 30$ cm, and consequently $y_0 \simeq 1.5$ cm. The total size of the inhomogeneous layer is $d_1 \simeq 3$-4 cm. The observed spectrum of $R(\lambda)$ in the range 3 cm $\leq \lambda \leq$ 100 cm is satisfied by the following data [35]:

$$\rho_1 = (0.6 - 0.7)\,g \cdot cm^{-3}, \quad \rho_2/\rho_1 = 1.3 - 1.5, \quad y_0 = 1.5\,cm.$$

Measurements of γ from the surface temperatures during eclipses and lunations also lead to the same degree of inhomogeneity. The difference between γ_1 and γ_2 likewise indicates a weak increase of the density with depth. The weak increase in the density of the substance with depth was likewise obtained from measurements carried out according to the Surveyor-VII program. In [121] it is indicated that the value $\rho_1 \simeq 1\ g \cdot cm^{-3}$ was obtained for the density of the surface substance; then the value increases with depth within the limits of the upper five centimeters to a value $\rho_2 \simeq 1.5\ g \cdot cm^{-3}$.

An investigation of the properties of the deeper layers of the moon turned out to be possible in connection with a peculiarity of the spectrum of the constant component of the integral radio emission obtained by the exact "artificial-moon" method. As indicated in §III.2 of this review, the fact that the constant component practically ceases to grow at $\lambda \geq 25$ cm is evidence of the increased density of the substance at the depth corresponding to a penetration depth 25-30 cm of the wavelengths (i.e., the spectrum of the constant component allows the thickness of the porous layer to be estimated). The theoretical curve plotted according to (23) is presented in Fig. 10. The same figure shows the experimental points taken from Fig. 21 for comparison purposes. It is evident that good agreement between the theoretical and experimental results is obtained for a thickness of the porous layer equal to

$$d_2 = 400 \pm 100\,cm$$

TABLE 3

Name of layer	Layer depth d, cm	Density ρ g · cm^{-3}	Porosity p, %	Thermal conductivity k(300) · 10^6, cal/(cm · sec · deg)	Specific heat c(300), cal/(g · deg)	Thermal inertia γ, cm^4 · sec$^{1/2}$/(cal deg)	Penetration depth of the thermalwave l_T, cm	Heat-flux density q · 10^6, cal /cm^2 · sec	Dielectric constant ε	Specific loss-angle tangent tan Δ/ρ	Penetration depth of the electromagnetic waves l_E, cm
									at centimeter wavelengths		
Porous surface	0—4	0,7±0,2	80	7±3	0,19	1000	7,5	0,7—0,8	2±0,2	9±3	15—17λ
Porous layer	4—400	$1^{+0,2}_{-0,1}$	60	9±3	0,19	800	7,5	0,7—0,8	2,5±0,2	8±2	15—17λ
Transition layer	400—600	1,5—2	30	10^3	0,19				3,5		
Rock layers	greater than 600	2,5—3	0—10	$5 \cdot 10^3$	0,19				5—6		

having a density $\rho_2 = 1$ g · cm^{-3} and a heat-flux density

$$q = (0.72 \pm 0.08) \cdot 10^{-6} \text{ cal} \cdot \text{cm}^{-2} \cdot \text{sec}^{-1}.$$

The spectrum of the reflection coefficient of radio waves also indicates a considerable increase in the density of the substance at a depth of the order of several meters. The growth of the reflection coefficient at wavelengths $\lambda > 10$ m [104] evidently is an indication of the fact that the reflection of these waves takes place from denser rock.

Figure 14 displays the theoretical spectra of the reflection coefficient which have been calculated for the following values of the parameters:

$$y_0 = 1.5 \text{ cm}; \quad \rho_1 = 0.7 \text{ g} \cdot \text{cm}^{-3}; \ \rho_2 = 1 \text{ g} \cdot \text{cm}^{-3}; \ \rho_3 = 2.5 \text{ g} \cdot \text{cm}^{-3}; \quad d_2 = 100, \ 200, \ 300 \text{ cm}.$$

The same figure shows the experimental points taken from Fig. 25 for comparison. It is evident that the surface-layer model considered provides a fairly good description of the observed spectrum of the reflection coefficient for the indicated values of ρ_1, ρ_2, ρ_3. For the thickness of the porous layer the value

$$d_2 = 200 \pm 100 \text{ cm},$$

is obtained. From radioastronomy measurements the value

$$d_2 = 400 \pm 100 \text{ cm},$$

is obtained. Evidently the latter is the more reliable of the two values. Actually, the information on the quantity d_2 in the spectrum of the reflection coefficient is basically carried by three measurements at wavelengths $\lambda > 10$ m; at the same time the accuracy of these measurements is low. In order to obtain d_2 reliably from the spectrum of $R(\lambda)$ one evidently requires additional radar data in the meter and decimeter wavelength ranges.

5. The Thermal Conductivity k and the Penetration Depth l_T of the Thermal Wave. Using the values $\gamma_1(300)$, $\gamma_2(300)$, ρ_1, ρ_2, c(300) obtained above, we find that the thermal conductivity of the substance forming the porous surface is $k_1(300) = (7 \pm 3) \cdot 10^{-6}$ cal · cm^{-1} · sec^{-1} · deg^{-1} and the thermal conductivity of the porous layer is $k_2(300) = (9 \pm 4) \cdot 10^{-6}$ cal · cm^{-1} · sec^{-1} · deg^{-1}. The values k_1 and k_2 given here for the thermal conductivities correspond to a temperature T = 300°K.

The penetration depth of the thermal wave is equal to

$$l_T = \left(\frac{2k}{\rho c \Omega}\right)^{1/2} \simeq 7.5 \text{ cm},$$

in accordance with (6).

6. The Electromagnetic Properties of the Substance: the Penetration Depth l_E of the Electrical Wave, the Dielectric Constant ε, the Specific Loss-Angle Tangent $\tan(\Delta/\rho)$. Above it was found that $l_E/l_T = 2.3\ \lambda$, $l_T \simeq 7.5$ cm; then $l_E \simeq 17\lambda$.

As has already been mentioned, several methods have been proposed for the determination of the dielectric constant ε of the substance forming the upper layer of the moon: from

the polarization of the intrinsic radiation [43-48, 102], from the distribution of the brightness temperature over the disk [37, 89, 101], from determining the delay of the phase of the radio emission of disk sectors situated at different longitudes along the lunar equator relative to the phase of the heating of these sectors [122], and from direct radar reflection measurements [104-108]. All of these methods are based on a lunar surface smooth enough that the Fresnel formulas are valid for the reflection coefficient.

The polarization method of determining ε was used in [43, 109, 123-125]. These measurements yield the value $\varepsilon_1 \simeq 2$ for the dielectric constant of the surface substance and $\varepsilon_2 \simeq 2.5$ for the dielectric constant of the substance making up the solid porous layer.

From the values found for ε we obtain the following values for the densities ρ_1 and ρ_2 in accordance with (31) and (32): $\rho_1 = 0.75$ g·cm^{-3} and $\rho_2 = 1$ g·cm^{-3}; these coincide with the values obtained above for these quantities from the spectra of the reflection coefficient and the constant component of the radio emission.

A comparison of the spectrum of the intensity variation during the lunar eclipses with the theoretical results allows the specific loss angle tangent $b_1 = \tan(\Delta_1/\rho_1)$ to be determined for the first few centimeters of the layer (see §III.3 of the review).

This value proves to be

$$b_1 = (9 \pm 3)\cdot 10^{-3}.$$

for centimeter wavelengths. Taking into account the values for c, γ_2, ε_2 obtained from lunation measurements, we have $b_2 = (8 \pm 2)\cdot 10^{-3}$.

7. The Chemical Composition of the Lunar Substance. In order to determine the chemical composition of the lunar substance the method described in §VII of the present review was used. Making use of the graph of Fig. 26 and the value $b = (9 \pm 3)\cdot 10^{-3}$ it is not difficult to find that the upper layer of the lunar substance has the following chemical composition on the average over a hemisphere:

$$SiO_2 - 57 \pm 3\%,\ Al_2O_3 - 16 \pm 1\%,\ Fe_2O_3 - 1 \pm 2\%,$$
$$FeO - 5 \pm 1\%,\ CaO - 5.5 \pm 2.5\%,\ MgO - 3{,}5 \pm 2\%,$$
$$Na_2O - 4 \pm 0.5\%,\ K_2O - 3 \pm 1\%,\ TiO_2 - 1 \pm 0.5\%.$$

Table 2 displays a comparison of the results of a chemical analysis obtained by the method indicated with the results of an analysis of the data obtained by the Surveyors [119] (the composition is expressed in percentage atomic content).

As is evident from the table, the agreement is very good. (In comparing the values for Ca it should be remembered that the data obtained by the Surveyors include the concentration of K.)

It is of interest to compare these results with the results of an analysis of the substance obtained by the astronauts of the Apollo-11 mission. The paper [63] presented the following average chemical composition of the lunar substance:

SiO_2—41%; CaO—10.5%; MgO—8%; FeO—18%; Al_2O_3—11.3%;
N_2O—0.6%; Ka_2O—0.2%; TiO_2—10%.

The difference between these data and the data given above is fairly substantial: considerably more iron, magnesium, and calcium oxides, and likewise an order more titanium dioxide. The substantially smaller amount of potassium and sodium oxides attracts attention. These features are explained by the authors of [63] on the basis of the evaporation of low-melting oxides during the process of the lunar thermal history.

8. The Microstructure of the Substance Forming the Upper Layer of the Moon. Above it is shown [13] that if the substance of the moon is impenetrable to infrared wavelengths, then the fraction of radiative radiation transfer through the pores is $k_{rn}/k_0 = 0.25$; for a penetrable substance it is $k_r/k_0 = 0.4$. Assuming $k = k_r + k_0 = (9 \pm 3)\cdot 10^{-6}$ cal·cm^{-1}·sec^{-1}·deg^{-1}, we find that $k_{rn} = (1.5\text{-}2.5)\cdot 10^{-6}$ cal·cm^{-1}·sec^{-1}·deg^{-1} or $k_r = (2.0\text{-}3.5)\cdot 10^{-6}$ cal·cm^{-1}·sec^{-1}·deg^{-1}.

From the value of k_{rn} obtained from (7) we find that the effective pore size is 170 to 350 μ. Since the porosity of the substance is close to 50%, the dimensions of the pores must be approximately equal to the size of the particles. If the substance is assumed penetrable to infrared rays, then in accordance with (8) it is found that a = 6-12 according to the value of k_r given; consequently, $l_E = (6\text{-}12)\lambda$ for infrared rays.

For wavelengths longer than 1000 μ, $l_E = 17\lambda$, as we have seen above. It seems to us most probable that the substance is impenetrable to infrared wavelengths. Then, in order for the heat transfer through the pores to be insignificant, the latter (and consequently the particles of the substance) must be many times as small as the mean free path of an infrared quantum which is equal to $l_E = 60\text{-}120$ μ. Evidently, these particles may have a size ranging from a tenth to several tenths of microns [13].

9. The Homogeneity of the Properties over the Surface. The results obtained above, with the exception of the data for γ, are averaged over the entire lunar hemisphere. Therefore, the question naturally arises as to the degree to which they correspond to local values. According to investigations performed at infrared wavelengths the thermal properties vary very little over the disk, with the exception of the bottoms of the radiant craters – by not more than 20 to 25% [126]. These variations are practically within the accuracy limits of the measurements. A high degree of homogeneity over the disk was likewise observed for such radioemission characteristics as $\overline{M}(\lambda)$ and $\overline{\xi}_1$ for averaging over areas ranging from tens to hundreds of kilometers [87-91, 126].

In this connection one can speak of the existence of a radiometric homogeneity that is similar to the well-known photometric homogeneity [127] that is associated with the homogeneity of the reflected-light characteristics. The radiometric homogeneity indicates homogeneity in the distribution of the electrical properties of the substance over the lunar surface in a layer having a thickness of at least 10 cm. In particular, it turns out that the substance on the surface of the seas and continents is practically identical [126]. The hypothesis that the upper rock of the continents is granite while the upper rock of the seas consists of basalt certainly does not correspond to the radiation characteristics.

More precise measurements of the distribution of the radioemission over the lunar disk at the wavelength $\lambda = 8$ mm [64] revealed a certain difference in the properties and allowed the conclusion to be drawn that the density of the substance forming the seas is evidently somewhat higher than the density of the substance forming the continents.

By virtue of the high homogeneity of the properties of the upper layer along the horizontal, the characteristics obtained represent the actual properties of the substance at each spot. The high homogeneity of the substances is substantiated by the results obtained by means of direct investigations of the moon. However, the investigations of the chemical composition according to the "Surveyor" program established that the seas contain 2-3 times more iron oxides than do the continents.

10. The Overall Model for the Structure of the Upper Layer of the Moon. On the basis of the above, it may be said that the upper layer of the moon can be described most completely by the four-layer model, although it is true that the density actually varies rather smoothly from layer to layer, so that subdivision into layers is introduced somewhat arbitrarily in order to simplify the picture. The properties of these layers are displayed in Table 3.

IX. Conclusion

As the consideration above has shown, an investigation of the intrinsic thermal radiation of the moon allows fairly complete data on the temperature mode of the lunar surface, its physical conditions, and the structure of the substance to be obtained. The objectivity of the data obtained is substantiated by the results of direct investigations of the moon. This allows it to be assumed reliably that the analysis method and the interpretations of the data may be successfully applied to the investigation of certain other planets (for example, Mars) the physical conditions of which are close to the physical conditions on the moon.

The authors thank V. D. Krotikov for his valuable discussion of the review.

LITERATURE CITED

1. E. Pettit and S. B. Nicholson, Astrophys. J., 72, 102 (1930).
2. R. H. Dicke and R. Beringer, Astropyys. J., 103, 735 (1946).
3. V. D. Krotikov and V. S. Troitskii, Usp. Fiz. Nauk, 81, 589 (1963).
4. V. S. Troitskii (Troitsky), J. Res. NBS, 69D, No. 12, 1585 (1965).
5. W. Horald, Solar System. Radio Astronomy, Athens, Ionospheric Institute National Observatory (1965), p. 295.
6. V. S. Troitskii, Izv. VUZ Radiofizika., 10, No. 9-10, 1266 (1967).

7. V. S. Troitskii, Phil. Trans. Royal Soc. London, A264, 145 (1969).
8. J. C. Wesselink, Bull. Astron. Inst. Neth., 10, 351 (1948).
9. J. G. Jaeger, Austr. J. Phys., 6, 10 (1953).
10. V. D. Krotikov and O. B. Shchukō, Astron. Zh., 40, 297 (1963).
11. V. S. Troitskii (Troitsky), A. B. Burov, T. N. Alyoshina, Icarus, 8, 423 (1968).
12. V. S. Troitskii, Astron. Zh., 31, 51 (1954).
13. V. S. Troitskii, Nature, 213, 688 (1967); V. S. Troitskii, Izv. VUZ, Radiofiz., 10, No. 8, 1051 (1967).
14. H. C. Ingrao, A. T. Young, and J. L. Linsky, Harv. Coll. Observ. Rep., No. 6 (1965).
15. R. W. Muncey, Nature, 181, 1458 (1958).
16. V. S. Troitskii, Astron. Zh., 39, 73 (1962).
17. V. A. Alekseev, L. V. Drobova, and V. D. Krotikov, Astron. Zh., 45, 1101 (1968).
18. W. J. Welch, D. D. Thornton, and S. Winter, J. Geophys. Res., 70, 2793 (1965).
19. V. S. Troitskii, Astron. Zh., 42, 1296 (1965).
20. E. Pettit, Astrophys. J., 91, 408 (1940).
21. R. W. Shorthill, J. M. Saary, Science, 150, 210 (1965).
22. A. E. Gear and J. A. Bastin, Nature, 196, 1305 (1962).
23. D. Buhl, PhD Thesis, University of California (1967).
24. T. Hagfors, J. Geophys. Res., 69, 3779 (1964).
25. B. G. Smith, J. Geophys. Res., 72, 4059 (1967).
26. H. C. Ingrao, A. T. Young, and J. L. Linsky, The Nature of the Lunar Surface, The Johns Hopkins Press, Baltimore (1966), p. 185.
27. J. J. Hopfield, Science, 151, 1380 (1966).
28. E. C. Roelof, Icarus, 8, 138 (1968).
29. T. V. Tikhonova and V. S. Troitskii, Astron. Zh., 46, 159 (1969).
30. A. M. Brekhovskikh, Waves in Laminar Media [in Russian], Izd. AN SSSR, Moscow (1957).
31. V. D. Krotikov, Izv. VUZ, Radiofiz., 6, No. 5, 889 (1963).
32. V. S. Troitskii, Izv. VUZ, Radiofiz., 5, No. 3, 602 (1962).
33. V. D. Krotikov and V. S. Troitskii, Astron. Zh., 40, 1076 (1963).
34. V. D. Krotikov and V. S. Troitskii, Izv. VUZ., Radiofiz., 6, No. 3, 633 (1963).
35. Yu. G. Matveev, G. L. Suchkin, and V. S. Troitskii, Astron., Zh., 42, 810 (1965).
36. V. D. Krotikov and V. S. Troitskii, Astron. Zh., 39, 1089 (1962).
37. V. A. Alekseev, T. N. Aleshina, V. D. Krotikov, and V. S. Troitskii, Astron. Zh., 44, 1070 (1967).
38. A. A. Bogdanov, I. Ya. Brusin, M. S. Kagorlitskii, and T. V. Tikhonova, Izv. VUZ., Radiofiz., 11, No. 6, 801 (1968).
39. T. V. Tikhonova and V. S. Troitskii, Astron. Zh., 46, 1324 (1969).
40. L. N. Bondar', K. M. Strezhneva, and V. S. Troitskii, Izv. Akad. Nauk, Fizika Zemli (in press).
41. V. A. Alekseev and V. D. Krotikov, Izv. VUZ, Radiofiz., 11, No. 8, 1133 (1968).
42. T. Hagfors and J. Moriella, Radio Science, 69D, 1614 (1965).
43. N. S. Soboleva, Astron. Zh., 39, 1124 (1962).
44. B. Ya. Losovskii, Astron. Zh., 44, 416 (1967).
45. N. S. Soboleva, Izv. GAO, No. 6, 205 (1967).
46. V. A. Alekseev, T. N. Aleshina, and V. D. Krotikov, Izv. VUZ, Radiofiz., 10, No. 5, 604 (1967).
47. V. A. Alekseev and V. D. Krotikov, Izv. VUZ, Radiofiz., 12, No. 1, 5 (1969).
48. V. A. Alekseev, T. N. Aleshina, V. D. Krotikov, and L. A. Mol'kova, Symposium on the Physics of the Moon and the Planets [in Russian], Kiev (1968).
49. D. Winter, Boeing Sci. Res. Lab. Doc., DI-82-0717 (1968).
50. B. C. Murray and R. L. Wildey, Astrophys. J., 139, 734 (1964).
51. F. J. Low, Astrophys. J., 142, 806 (1965).
52. R. W. Shorthill and J. M. Saary, Boeing Sci. Res. Lab. Doc., DI-82-0778 (1969).
53. J. M. Saary and R. W. Shorthill, Icarus, 2, 115 (1963).
54. K. J. K. Buettner, Planet. Space Sci., 11, 135 (1963).
55. J. A. Bastin, Nature, 297, 1381 (1965).
56. P. G. Messger and H. Strassl, Planet. Space Sci., 1, 213 (1959).
57. V. D. Krotikov, V. A. Porfir'ev, and V. S. Troitskii, Izv. VUZ, Radiofiz., 4, No. 6, 1004 (1961).
58. N. M. Tseitlin, Izv. VUZ, Radiofiz., 6, No. 6, 1265 (1963).

59. T. V. Tikhonova, Izv. VUZ, Radiofiz., 12, No. 8, 1121 (1969).
60. L. N. Bondar', M. R. Zelinskaya, V. A. Porfir'ev, and K. M. Strezhneva, Izv. VUZ, Radiofiz., 5, No. 4, 802 (1962).
61. B. N. Semenov, S. A. Kamenskaya, V. S. Troitskii, and V. M. Plechkov, Izv. VUZ, Radiofiz., 5, No. 5, 882 (1962).
62. V. D. Krotikov, Izv. VUZ, Radiofiz., 5, No. 3, 604 (1962).
63. Science, 165, No. 3899, 1211 (1969).
64. V. D. Krotikov and V. A. Porfir'ev, Izv. VUZ, Radiofiz., 6, No. 2, 242 (1963).
65. V. D. Krotikov, Izv. VUZ, Radiofiz., 6, No. 6, 1087 (1963).
66. D. A. Dmitrenko, S. A. Kamenskaya, and V. L. Rakhlin, Izv. VUZ, Radiofiz., 7, No. 3, 555 (1964).
67. A. V. Zakharov, V. D. Krotikov, V. S. Troitskii, and N. M. Tseitlin, Izv. VUZ, Radiofiz., 7, No. 3, 553 (1964).
68. V. D. Krotikov, V. S. Troitskii, and N. M. Tseitlin, Astron. Zh., 41, No. 5, 951 (1964).
69. V. A. Alekseev, V. D. Krotikov, Yu. G. Matveev, N. B. Mikhailova, V. A. Porfir'ev, V. P. Ryazanov, A. I. Sergeeva, K. M. Strezheva, V. S. Troitskii, and S. A. Shmulevich, Izv. VUZ, Radiofizka, 9, No. 5, 1030 (1966).
70. V. M. Plechkov, Astron. Zh., 44, No. 1, 154 (1967).
71. V. A. Alekseev, L. N. Bondar', S. A. Kamenskaya, V. D. Krotikov, Yu. G. Matveev, K. M. Strezhneva, and V. S. Troitskii, Astron. Zh., 44, No. 3, 593 (1967).
72. J. H. Piddington and H. G. Minnet, Austr. J. Sci. Res., 2A, 643 (1949).
73. J. P. Hagen, NRL Report No. 3504 (1949).
74. J. H. Piddington and H. G. Minnet, Austr. J. Sci. Res., 4A, 459 (1951).
75. V. S. Troitskii and M. R. Zelinskaya, Astron. Zh., 32, No. 6, 550 (1955).
76. A. E. Solomonovich, Astron. Zh., 35, No. 1, 129 (1958).
77. M. R. Zelinskaya, V. S. Troitskii, and L. I. Fedoseev, Astron. Zh., 36, No. 4, 643 (1959).
78. M. R. Zelinskaya, V. S. Troitskii, and L. I. Fedoseev, Izv. VUZ, Radiofiz., 2, No. 3, 506 (1959).
79. A. G. Kislyakov, Izv. VUZ, Radiofizika, 4, No. 3, 433 (1961).
80. K. M. Strezhneva and V. S. Troitskii, Izv. VUZ, Radiofiz., 4, No. 4, 600 (1961).
81. W. J. Medd and N. W. Broten, Planet. Space Sci., 5, 307 (1961).
82. A. G. Kislyakov, Astron. Zh., 38, No. 3, 561 (1961).
83. V. S. Troitskii, V. D. Krotikov, and N. M. Tseitlin, Astron. Zh., 44, No. 2, 413 (1967).
84. A. I. Naumov, Izv. VUZ, Radiofiz., 6, No. 4, 847 (1963).
85. L. I. Fedoseev, Izv. VUZ, Radiofiz., 6, No. 4, 655 (1963).
86. V. A. Razin and V. T. Fedorov, Izv. VUZ, Radiofiz., 6, No. 5, 1052 (1963).
87. V. N. Koshchenko, A. D. Kuz'min, and A. E. Solomonovich, Izv. VUZ, Radiofiz., 4, No. 4, 596 (1961).
88. A. E. Solomonovich and V. N. Koshchenko, Izv. VUZ, Radiofiz., 4, No. 4, 591 (1961).
89. A. E. Solomonovich and B. Ya. Losovskii, Astron. Zh., 39, No. 6, 1074 (1962).
90. A. E. Solomonovich, Astron. Zh., 39, No. 1, 79 (1962).
91. A. G. Kislyakov and A. E. Solomonovich, Izv. VUZ, Radiofiz., 6, No. 3, 431 (1963).
92. A. E. Solomonovich, Proc. Roy. Soc., 296, 354 (1967).
93. C. H. Mayer, R. M. McCullough, and R. M. Sloanaker, The Solar System, Vol. 3, University of Chicago (1961).
94. J. E. Gibson, Astrophys. J., 133, 1072 (1961).
95. W. M. Sinton, Astrophys. J., 123, No. 2, 325 (1956).
96. R. W. Shorthill, H. C. Borough, and J. M. Canley, Publ. Astron. Soc. Poc., 72, No. 429, 481 (1960).
97. J. P. Castelli, C. P. Ferioli, and J. Aarons, Astronom. J., 65, No. 9, 485 (1960).
98. J. M. Saary and R. W. Shorthill, Boeing Sci. Res. Lab., July (1962).
99. S. A. Kamenskaya, A. G. Kislyakov, V. D. Krotikov, V. M. Plechkov, A. I. Naumov, V. N. Nikonov, V. A. Porfir'ev, K. M. Strezhneva, V. S. Troitskii, L. I. Fedoseev, L. V. Lubyako, and É. P. Sorokina, Izv. VUZ, Radiofiz., 8, No. 2, 219 (1965).
100. V. M. Plechkov, Astron. Zh., 43, No. 1, 172 (1966).
101. V. N. Koshchenko, A. D. Kuz'min, and A. E. Solomonovich, Izv. VUZ, Radiofiz., 4, No. 4, 596 (1961).

102. V. S. Troitskii and N. M. Tseitlin, Izv. VUZ. Radiofiz., 3, No. 6, 1127 (1960).
103. J. V. Evans, Physics and Astronomy of the Moon, Academic Press, New York–London (1962), p. 429.
104. J. V. Evans, J. Res. Nat. Bur. Stand., 69D, No. 12, 1637 (1965).
105. A. Giraund, J. Res. Nat. Bur. Standards, 69D, No. 12, 1677 (1965).
106. J. R. Davis, D. C. Rahlfs, G. A. Skaggs, and J. W. Joss, J. Res. Nat. Bur. Standards, 69D, No. 12, 1659 (1965).
107. J. V. Evans and T. Hagfors, J. Geophys. Res., 71, No. 20, 4871 (1966).
108. T. Hagfors, in: Symposium on the Physics of the Moon and the Planets [in Russian], Kiev (1968).
109. R. D. Davies and F. F. Gardner, Aust. J., 19, No. 16, 823 (1966).
110. N. P. Barabashovand A. T. Chekirda, Astron. Zh., 3, 827 (1960).
111. B. Hapke and V. Han Horn, CRSR 1939, Cornell University, Ithaca, New York, February (1963).
112. B. Hapke, Astron. J., 71, 333 (1966).
113. B. Lyot, Ann. de J'Obs. de Paris, Sect. de Medon, 8 (1929).
114. A. Dollfus, Ann. Astrophys., 19, No. 2 (1956).
115. V. D. Krotikov, Izv. VUZ, Radiofiz., 5, No. 6, 1057 (1962).
116. W. E. Fensler, E. F. Knott, A. Olte, and K. M. Siegel, IAU Symposium, Academic Press., New York–London (1962), p. 14.
117. A. Olte and K. M. Siegel, Astrophys. J., 133, 706 (1961).
118. A. G. Betekhtin, Course in Minerology [in Russian], Izd. GNT, Moscow (1966).
119. V. S. Troitskii, L. N. Bondar', M. R. Zelinskaya, and K. M. Strezhneva, Astron. Vestnik, 3, No. 4 (1969).
120. N. N. Kurpenio, Dissertation [in Russian], IKI AN SSSR (1969).
121. Leonard Jaffe, Science, 164, 1514 (1969).
122. V. S. Troitskii, Astron. Zh., 38, 1001 (1961).
123. G. E. Heiles and F. D. Drake, Icarus, 2, 281 (1963).
124. Gol'nev and N. S. Soboleva, Pros. Astr. Obs. Pulkova, 13, 83 (1964).
125. J. W. Baars, P. G. Mezger, N. Savin, and H. Wendker, Astr. J., 70, 132 (1965).
126. V. S. Troitskii, Astron. Zh., 59, 724 (1964).
127. N. P. Barbashov, V. A. Ezerskaya, V. I. Ezerskii, and T. I. Ishutina, Izv. Kom. po Fiz. Planet, No. 1, 67 (1959).
128. M. J. Campbell, J. Ulrichs, and B. Hapke, CRSR, Cornell University, Ithaca, New York, February (1969).
129. J. L. Linsky, Icarus, 5, No. 6, 606 (1966).
130. L. D. Stimpson and J. W. Lucas, Report JPR No. NAS 7-100 (1968).
131. L. I. Fedoseev, L. V. Lubyako, and L. M. Kukin, Izv. VUZ, Radiofiz., 11, No. 6, 807 (1968).
132. A. G. Kislaykov and V. M. Plechkov, Izv. VUZ, Radiofiz., 7, No. 1, 46 (1964).
133. J. A. Waak, Astron. J., 66, 298 (1961).
134. J. E. Baldwin, Month. Not. Roy. Astron. Soc., 122, 513 (1961).